The ER Quality Control of human ether-a-go-go related gene (KNCH2) Ion Channel

Brittany Williamson

Department of Biochemistry
McGill University
Montreal, Quebec, Canada

July, 2016

A thesis submitted to McGill University in partial fulfillment of the requirements of the degree of Master of Science in Biochemistry

Abstract

The functional expression of hERG/Kv11.1 K^+ channel in cardiac myocytes is important for regulated heart rhythm. Inherited Long-QT Syndrome type-2 (LQT2) is caused by mutations in hERG, resulting in impaired cardiac repolarization and increased risk of fatal ventricular arrhythmias. Of the numerous autosomal dominant LQT2 mutations found in hERG, several cause the misfolding of hERG and the subsequent abnormal trafficking from the endoplasmic reticulum (ER) to the plasma membrane (PM). The cellular protein quality control system is central to hERG expression and the proper folding of hERG is dependent on chaperones Hsp90 and Hsp70 (1). Misfolded wild-type and mutant hERG are cleared from the ER by ER-associated proteasomal degradation (ERAD). This requires the targeting of misfolded substrate, where ubiquitin must be transferred from an E2 enzyme to the substrate through an E3 ligase (2). Previously, Hsp70 was shown to be involved in hERG ERAD through its co-chaperone, the E3 ligase CHIP (3). More recent work in our lab however, identified TRC8 to be a potential quality control E3 ligase that recognizes misfolded hERG and promote ERAD. Here, we find TRC8 knockdown rescues hERG by ~25%, while the overexpression inhibits hERG maturation and trafficking, shown by Western blotting, pulse chase assays, and patch clamping. When co-transfected with wild-type hERG, wild-type and mutant TRC8 also immunoprecipitate, as shown by Western blot. Though the ubiquitination of hERG and degradative effect is only seen with wild-type TRC8, we believe that there may be a transmembrane spanning area where TRC8 and hERG interact prior to ubiquitination and subsequent ERAD. Furthermore, a drug-induced structurally stabilized mutant hERG is able to evade TRC8 degradation, indicating that TRC8 acts as a quality control E3 ligase.

We think that ERAD translocon member and ligase partner, Derlin-1, may also complete part of the hERG ERAD complex. In order to better distinguish the folding and degradative mechanisms of hERG, we hope to identify additional ERAD components that work with TRC8 to remove misfolded hERG. Understanding the proteins that make up the degradative pathway of hERG will be advantageous in developing potential LQT2 therapies.

Résumé

L'expression fonctionnelle du canal hERG/Kv11.1 K^+ dans les myocytes cardiaques est importante pour un rythme cardiaque régulé. Long-QT Syndrome type-2 (LQT2) hérité, est causé par des mutations dans hERG, résultant en une repolarisation cardiaque réduite et un risque d'augmentation d'arythmie ventriculaire mortelle. Des nombreuses mutations LQT2 autosomiques dominantes trouvées dans hERG, plusieurs causent le mauvais repliement de hERG et par conséquent le trafic anormal du réticulum endoplasmique (RE) jusqu'à la membrane plasmique (PM). Le système qui contrôle la qualité de la protéine au niveau cellulaire est central pour l'expression de hERG et le bon repliement de hERG est dépendant des chaperons Hsp90 et Hsp70 (1).Un mauvais repliement de hERG de type sauvage et mutante sont éliminés du RE par le réticulum endoplasmique dégradations-Associated (ERAD). Ceci nécessite le ciblage du substrat au mauvais repliement où l'ubiquitine doit être transférée d'une enzyme E2 au substrat par une ligase E3 (2). Il a été montré auparavant que Hsp70 est impliqué dans hERG ERAD par son co-chaperon, la ligase E3 CHIP (3). Cependant, la recherche la plus récente effectuée dans notre laboratoire a identifié TRC8 comme étant une ligase E3 contrôle de qualité potentiel qui reconnaît hERG mal repliée et qui stimule ERAD. Ici, nous constatons que la diminution de l'expression de TRC8 (KD) sauve hERG de ~25%, tandis qu'une surexpression de TRC8 réfrène la maturation et le trafic de hERG, démontré par buvardage Western, et marquage court avec chasse. De plus, TRC8 type sauvage et mutante immunoprécipitent quand ils sont co-tranfectés avec hERG type-sauvage, ce qui est révélé par buvardage Western. Bien que l'ubiquitination de hERG et l'effet de dégradation soient seulement observés avec TRC8 type sauvage, on croit qu'il

existe une zone transmembranaire où TRC8 et hERG interagissent avant l'ubiquitination et l'ERAD subséquent. En outre, une hERG mutante structurellement stabiliser par des drogues est capable d'échapper la dégradation de TRC8, indiquer que TRC8 se comporte comme un E3 ligase contrôle qualité. On pense que le membre translocon de ERAD et partenaire ligase Derlin-1, peut aussi compléter une partie du complexe hERG ERAD. Pour améliorer notre compréhension du repliement et du mécanisme de dégradation de hERG, on espère identifier d'autres composantes de ERAD qui travaillent avec TRC8. Comprendre les protéines qui composent la voie de dégradation de hERG sera avantageux pour le développement potentiel de traitements du LQT2.

Acknowledgements

Many relationships have encouraged my progress at McGill and have left me a more confident scientist, intelligent student, and well-rounded individual. I would like to thank the Department of Biochemistry from which I received funding, the community of McGill University, and first floor Bellini, among especially influential people, which I will list here.

First and foremost, I would like to thank my two supervisors, Jason C. Young and Alvin Shrier. I would not have been able to complete this work without your scientific input or your kind words of enthusiasm. I am lucky to have been a part of both of your labs. In addition to the Young and Shrier lab members, I would also like to give a special thanks to Patrick Kim Chiaw who was my mentor and confidant- our conversations over coffee encouraged my progress.

My advisory committee: For giving useful insight, being available for guidance, and for supporting my project.

My Mom, Dad, three fabulous sisters, extended family members and friends: for understanding my demanding schedule, for video calling me during missed holidays, for paying my flights home, for the kind letters, and for filling me with love with every email, phone call, and visit that we shared. I love you to the moon and back.

For my new friends on first floor Bellini: for providing scientific vision, stimulating conversation, and much-needed happy hour.

Preface and Contribution of Authors

The content of this work is to be published with a manuscript in preparation.

The contributions for this thesis work involved collaborations with a previous PhD student in our laboratory, Christine Hantouche, and a member of the Shrier lab, Joshua Solomon. Christine Hantouche showed the restoration of hERG when TRC8 was knocked down in the initial siRNA screen (Figure 2.1A). Joshua Solomon completed the patch clamp experiments (Figure 2.3C). I performed and analyzed all additional experiments with supervision and project design from Dr. Young and Dr. Shrier.

Table of Contents

Abbreviations and Acronyms

ADP	Adenine-nucleotide di-phosphate
ATP	Adenine-nucleotide tri-phosphate
CF	Cystic Fibrosis
CNX	Calnexin
CRT	Calreticulin
ECG	Electrocardiogram
EDEM	ER degradation-enhancing α-mannosidase-like protein
ER	Endoplasmic reticulum
ERAD	Endoplasmic reticulum-associated degradation
FG	Fully glycosylated
GA	Golgi apparatus
GLsI	Glucosidase I
GlsII	Glucosidase II
hERG	Human ether-a-go-go related gene
HMG CoA	3-hydroxy-3-methylglutaryl coenzyme A
HO-1	Heme Oxygenase-1
LQTS	Long QT Syndrome
NAFLD	Non-alcoholic fatty liver disease
NEF	Nucleotide exchange factor
Npl4	Nuclear protein localization 4
OST	Oligosaccharyltransferases
p97	Valosin-containing protein
QC	Quality control
RING	Really interesting new gene
SREBP	Sterol regulatory element-binding protein
TRC8	Translocation in renal carcinoma, chromosome 8 gene
Ufd1	Ubiquitin fusion degradation 1
UGT1	UDP-glucose: glycoprotein glucosyltransferase 1
UPR	Unfolded protein response
UPS	Ubiquitin proteasome system
VF	Ventricular Fibrillation

List of Figures

Chapter 1

General Introduction

Sudden Cardiac Death And Long QT Syndrome

Millions of Canadians are affected by cardiovascular disease, making it the most costly disease in Canada with over $2 billion in direct costs spent every year [1]. In particular, sudden cardiac death claims the lives of hundreds of thousands of North Americans every year and can be attributed to the presence of irregular heart rhythms called arrhythmias. Ventricular fibrillation (VF) is the most common diagnosed arrhythmia found in cardiac arrest patients. In VF, the regulated systematic contraction of the ventricular myocardium is taken over by a high frequency, uncoordinated excitation resulting in premature contraction of the ventricle [2]. This dysfunctional contraction prevents the pumping of blood and results in sudden death. VF can be caused by structural heart disease or by ion channel aberrations, such as that seen with long QT syndrome (LQTS) [3].

LQTS is an inherited cardiac disorder that causes syncope, seizures, and sudden death in usually healthy individuals. Most LQT gene carriers have a visible prolongation of the QT interval seen on an electrocardiogram (Figure 1.1). Prolonged repolarization between heartbeats can produce ventricular arrhythmias such as *torsade de pointes*, named as such due to the distinctive waxing and waning of the QRS peak on the electrocardiogram [4]. While *torsade de pointes* may terminate independently, these arrhythmias can further degenerate into ventricular fibrillation and sudden death [5].

The long QT interval present in LQTS patients is related to changes in the QT interval of the electrocardiogram (ECG). The prolongation of the QT interval is directly related to the ventricular action potential, which is generated by the flow of ions through ion channels in the cell membrane of the ventricular cells. The phases of the ventricular action potential coincide with distinct waves and intervals seen on the ECG (Figure 1.1). The ventricular action potential is made up of five phases. It begins with the initial rapid depolarization caused by the opening of Na^+ channels (phase 0). This is followed by an initial rapid repolarization phase caused by the rapid opening of transient outward potassium channels (phase 1). A plateau phase follows, which is due to the balance of inward Ca^{2+} current and the repolarizing outward K^+ currents (Phase 2). The slow delayed rectifier K^+ current (I_{Ks}) and the rapid delayed rectifier K^+ current (I_{Kr}) together make up the K^+ current in Phase 2. Phase 3 is due to the increase of the delayed rectifier currents and a decrease in the Ca^{++} that returns the cell to the resting potential (phase 4) (Figure 1.1). In cardiac myocytes, the human ether-a-go-go related gene (hERG/Kv11.1/KCNH2) channel is responsible for the rapid delayed rectifier potassium current in phase 3 of the ventricular action potential and contributes to ventricle repolarization. Predictably, mutations in hERG cause the reduced functional expression of the hERG channel and a reduction in the I_{Kr} current. This results in delayed ventricular repolarization, a prolonged QT interval seen on the ECG associated with the clinical presentation of LQTS [6].

Figure 1.1: Electrocardiogram and Ventricle Action Potential

Electrocardiogram (ECG), with significant transitions in the heart indicated by letters PQRST. The P wave reflects atrial depolarization, QRS indicates ventricular depolarization and the T wave represents the ventricular repolarization. Below indicates the ventricular action potential. Phase 0 is in line with the ventricular repolarization, a plateau phase 2 and the ventricular repolarization is seen at phase 3. Figure obtained from [7].

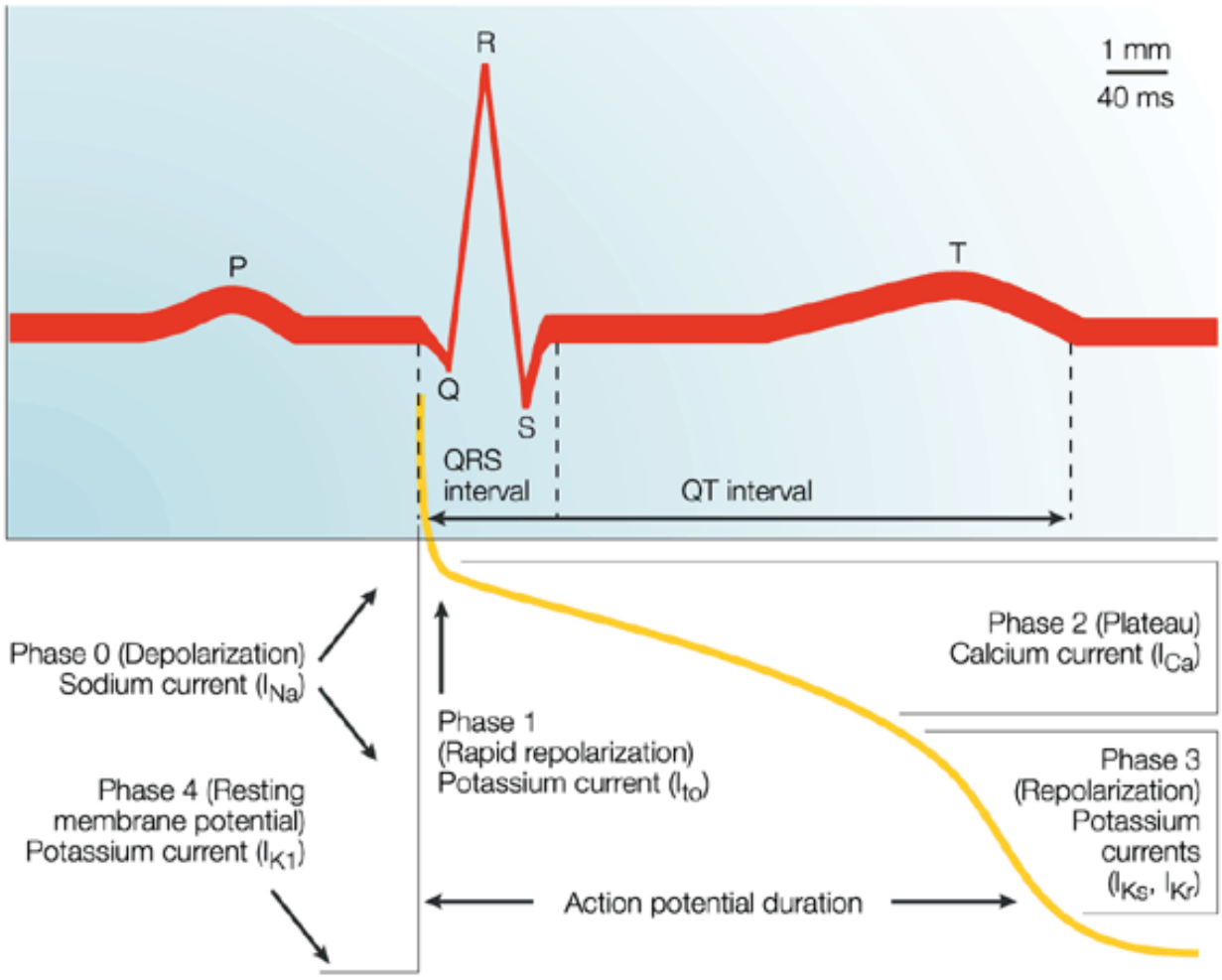

Nature Reviews | Drug Discovery

Human Ether a-go-go related gene (hERG)

hERG is a voltage dependent channel that is activated by depolarization and allows potassium ions to pass through the channel, which is made from the four tetramerized alpha subunits (Figure 1.2). Similar to other members of the voltage gated potassium channel (Kv) family, each subunit has six transmembrane domains (S1-S6), where S1-S4 contain the voltage sensing region and S5-S6 forms the pore (Figure 1.2) [8]. The longer isoform, hERG1a, consists of these membrane-spanning helices in addition to large cytosolic domains on each subunit: the cyclic-nucleotide-binding domain (CNBD) at its C-terminus and a Per-Arnt-Sim (PAS) domain at its N-terminus. The shorter isoform, hERG1b, lacks the N-terminus PAS domain and has a shorter unrelated sequence instead. Tetramers of hERG1a alone can form functional channels while tetramers of hERG1b cannot, and most studies in cell lines use hERG1a. However there is some evidence that heteromers of hERG1a and 1b may form the physiologic channel in human cardiomyocytes [9, 10].

Figure 1.2: hERG 1a and 1b gene and hERG structure

The hERG 1a protein contains a Per-Arnt-Sim (PAS) domain, 6 transmembrane domains, and a cyclic nucleotide binding domain (cNBD) whereas hERG1b maintains the cNBD and the transmembrane region but lacks the PAS domain. hERG channels form in tetramers to pass potassium ions through.

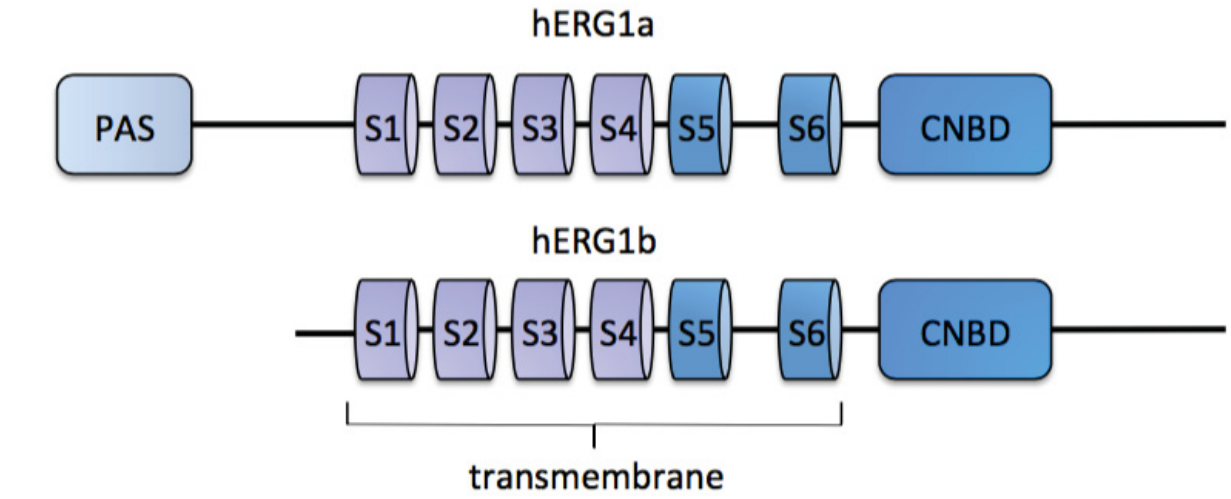
hERG1a
PAS
S1
S2
S3
S4
S5
S6
CNBD
hERG1b
S1
S2
S3
S4
S5
S6
CNBD
transmembrane

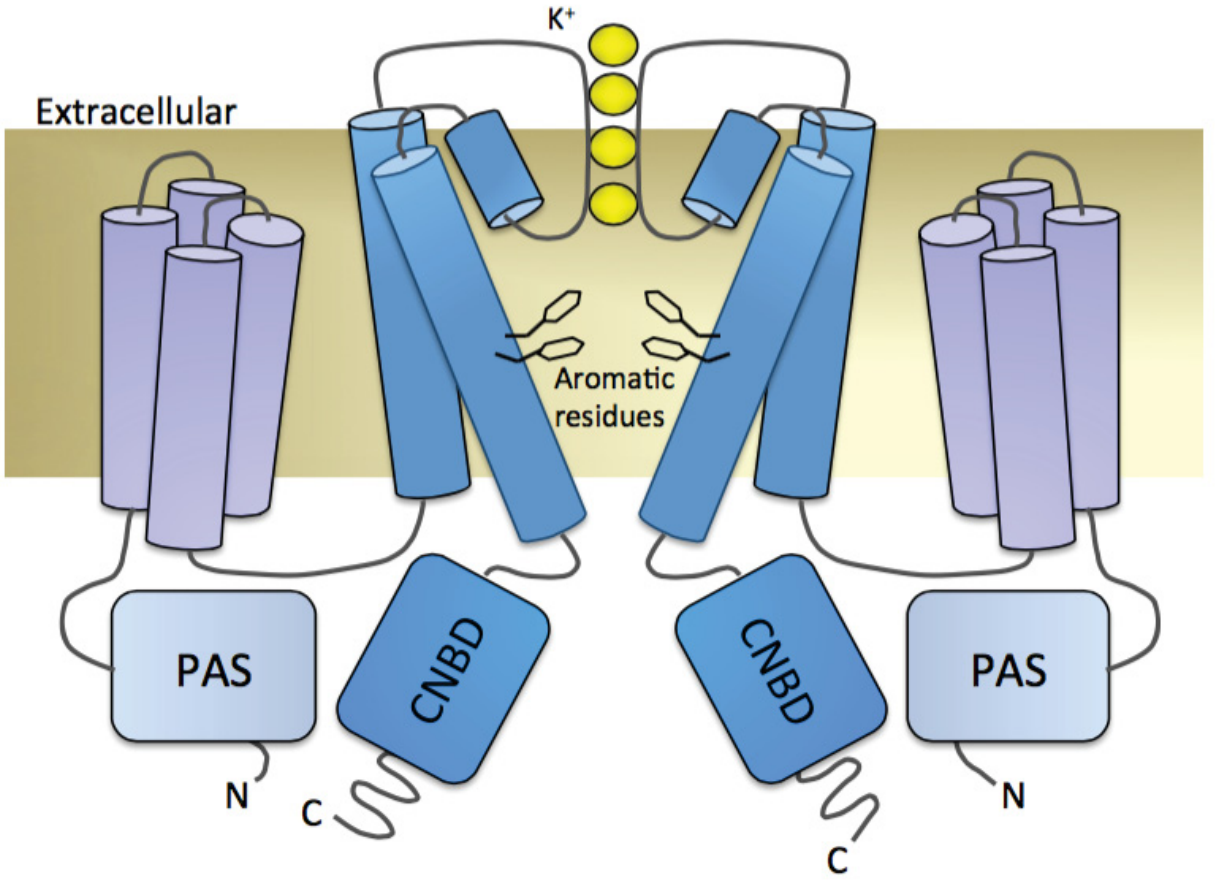
K+
Extracellular
Aromatic
residues
PAS
CNBD
CNBD
PAS
N
C
C
N

hERG Trafficking

In hERG biogenesis, the protein quickly forms a tetramer in the endoplasmic reticulum (ER) membrane, where it becomes N-linked glycosylated. Molecular chaperones aid the folding of hERG, and once properly folded, hERG traffics to the Golgi apparatus where it becomes complex glycosylated. Consequently hERG can proceed to traffic to the cell surface and function as a potassium ion channel (Figure 1.3).

There are two forms of the disease, acquired LQT2 and inherited LQT2, both which exhibit less functional hERG found at the plasma membrane caused by drug, or gene mutations, respectively [11]. Blocking of the hERG pore, or modifying the cellular processing by preventing exit from the ER, can cause a decrease of functional hERG. The hERG channel is sensitive to unintended drug binding and manipulation of its cellular processing, and these off-target drug-induced arrhythmias result in a major proportion of drug withdrawal from the market [12, 13]. Also, the sensitivity to drugs of hERG processing and stability at the plasma membrane is a unique area of quality control that remains to be fully explored.

Figure 1.3: hERG secretory pathway

hERG is synthesized in the ER, is core glycosylated and trafficked to the Golgi where its glycosylation is modified, and then to the cell surface. The channel can be degraded at the ER if improperly folded, or it can go through internalization from the PM, recycling and lysosomal degradation.

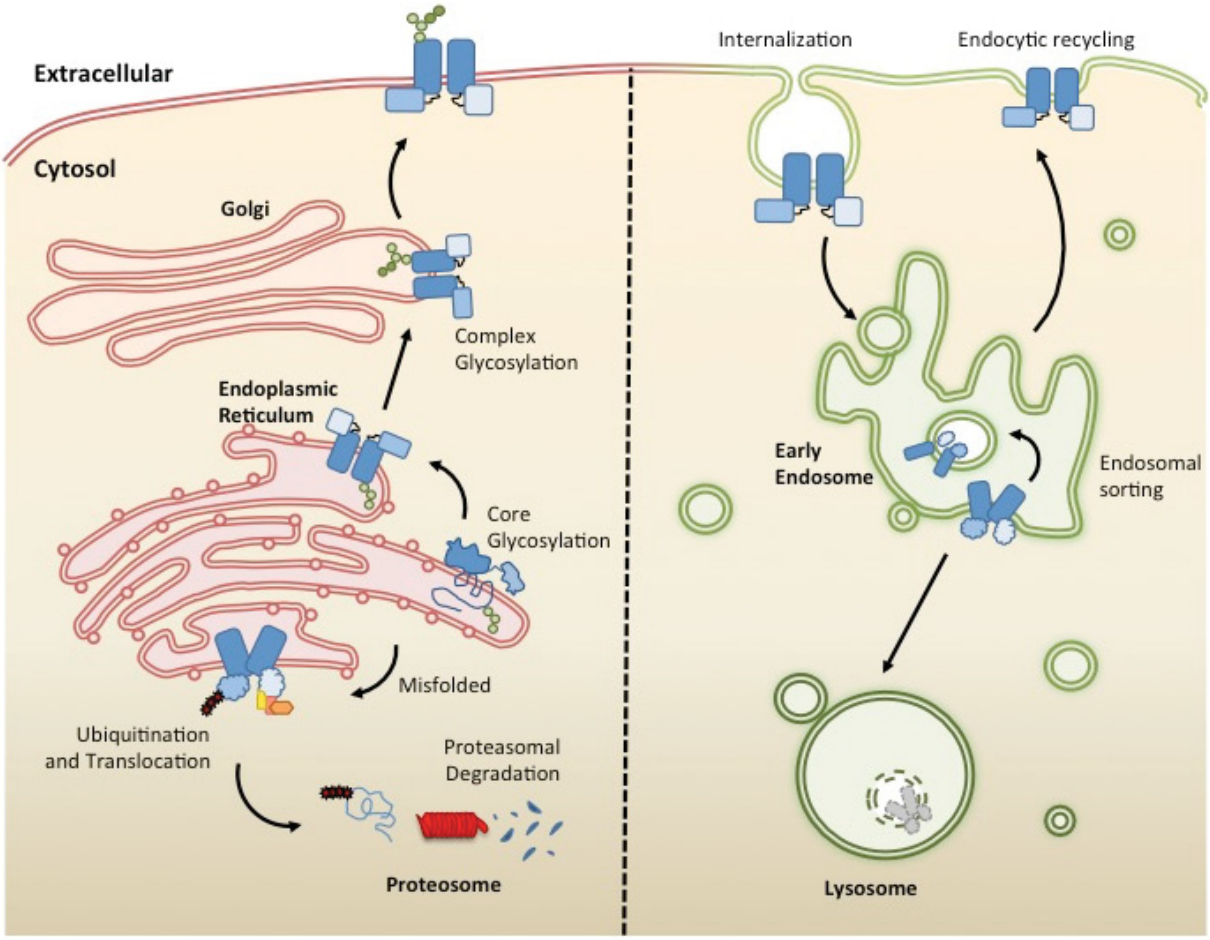
Extracellular
Cytosol
Golgi
Complex
Glycosylation
Endoplasmic
Reticulum
Core
Glycosylation
Misfolded
Ubiquitination
and Translocation
Proteasomal
Degradation
Proteosome
Internalization
Endocytic recycling
Early
Endosome
Endosomal
sorting
Lysosome
Biosynthesis and maturation
Turnover at cell periphery

Several hundred mutations in hERG result in inherited LQT2, which has a prevalence of 1:6000 [14]. A large majority of the mutants found in LQT2 are missense mutations and result in impaired ER exit, accelerated degradation, and reduced plasma membrane (PM) surface hERG expression. The variability between severity of mutation effects is broad; some mutants have a mild defect of maturation while others completely abolish formation of a fully glycosylated form of hERG [15, 16]. Experimentally, restoration of hERG trafficking from the ER to the cell surface can for some mutants be accomplished with drug stabilizers or by lowered temperature. Unfortunately, these systems are unsuitable for clinical treatment since they typically result in the blocking of hERG or provide a physiologically irrelevant experimental system. Drug screening of pharmaceuticals that both enhance the maturation of hERG and allow proper potassium channel activity still must be completed. To date, these obstacles have led to the emphasis on understanding the folding and trafficking pathways of hERG, which may be manipulated to restore detrimental inherited mutations.

hERG Quality Control Network

For hERG to be expressed at the cell surface it must first undergo proper folding of the polypeptide chain, post-ribosomal release, post-translational folding, and proper assembly into a tetramer. The ER quality control (QC) system maintains a homeostasis of folded proteins, and hERG processing in particular relies on folding mechanisms completed by molecular chaperones, which includes Hsp70 and Hsp90 [17].

In hERG biosynthesis, molecular chaperones promote a properly folded hERG in the ER membrane, which is followed by tetramerization of the oligomers, N-linked

glycosylation, and final transport to the Golgi apparatus. At the Golgi, hERG gains another 20 kDa of glycosylation, and this 155 kDa form of hERG represents the fully glycosylated (FG) pool of protein that will either transport to the cell surface, remain in the Golgi, or become recycled by endosomes before lysosomal degradation (Figure 1.3).

Protein Homeostasis

Normal function of the cell relies on the proper activity and folding of its large network of proteins. Close to a third of the cell's proteins are synthesized in the ER and consist of secretory proteins. As such, regulation of folding and trafficking mechanisms must be robust [18]. In eukaryotes, nearly all secretory proteins are translocated across the ER membrane and are trafficked from the ER to the Golgi soon after their synthesis. During protein synthesis, the polypeptide enters the ER where signal sequences are cleaved, sugar moieties are added, and the protein folds. To complete folding, the ER contains chaperones, co-chaperones, glycan-modifying enzymes and lectins, which all support the formation of a native secondary structure of the amino acid sequence. Upon proper folding, secretory proteins are incorporated into transport vesicles and fuse with the *cis* Golgi network. These proteins move by cisternal migration to then be secreted from the *trans* face of the Golgi, where a final secretory vesicle will take these proteins from the Golgi and fuse with the plasma membrane through exocytosis [19].

In a misfolded state, proteins can aggregate and potentially become cytotoxic to the cell, which is seen in a variety of protein misfolding diseases. In order to prevent cell toxicity and the induction of ER stress, it is crucial for the cell to properly fold the many proteins that range in structural and oligomeric diversity. To this means, the cell has

developed rigorous protein quality control (QC) machinery to ensure that properly folded proteins can be made while incorrectly folded proteins do not accumulate to create stress and form toxic aggregates. The ER QC system consists of molecular chaperones to promote folding, and alternate machinery to initiate degradation.

Folding Machinery

In order to keep up with polypeptide synthesis and to maintain protein homeostasis, newly made polypeptides must be folded so that they can exit the ER and prevent accumulation of substrates. The ER folding machinery is made up of chaperones that are involved in folding both newly synthesized proteins and misfolded substrates. Chaperones resident in the lumen of the ER act specifically on secretory proteins, while chaperones in the cytosol act on cytosolic domains of secretory proteins, such as those found in hERG [20]. ER quality control relies on the chaperone system to encourage protein folding, oligomerization, and post-translational modifications. The main chaperones involved in this quality control system are heat shock proteins Hsp70 and Hsp90, and the carbohydrate-binding chaperones. These protein families form cooperative networks in cells and participate in several stages of protein biogenesis so that the cell obtains functional proteins and the accumulation of misfolded proteins can be prevented [20].

Chaperones

Chaperones recognize unfolded substrate to prevent aggregation, and in some cases promote subsequent folding through ATPase-driven cycles of binding and release. Some chaperones recognize exposed hydrophobic and cysteine residues that are normally buried in the protein but are found externally on aberrant proteins. For the ATP-dependent chaperones, binding to substrate is regulated through a step-wise process of ATP binding and hydrolysis, which allows chaperones to assist the correct folding of substrates. The main families of ATP-dependent chaperones that encourage the folding of ER substrates are Hsp70 and Hsp90 families. The cytosolic forms are most relevant for hERG and will be the main focus.

Hsp70 Family

Hsp70 proteins are constitutively active as they are essential for preventing aggregation of misfolded proteins and maintain homeostasis in non-stress conditions [21]. The Hsp70 substrate binding cycle consists of the chaperone binding and releasing short hydrophobic segments within the substrate, which is caused by a conformational change in Hsp70 during its ATP-hydrolytic reaction regulated by co-chaperones (Figure 1.4). All Hsp70 family members have common structural features including a nucleotide-binding domain (NBD) with ATPase activity, and a C-terminal substrate-binding domain (SBD), which is joined to the NBD by a conserved linker. Hsp70 will cycle between a high substrate affinity (ADP-bound) state and a low substrate affinity (ATP-bound) state. The switch between ATP and ADP provides conformational changes and Hsp70 will

either clamp down on substrate or open up for release, and multiple cycles of substrate binding promote folding [22-26].

In order to progress efficiently through the ATPase cycle, Hsp70 requires the input of co-chaperones in the Hsp40 (DNAJ) family, and nucleotide exchange factors (NEFs). In the Hsp70 cycle, Hsp40 co-chaperones stimulate the hydrolysis of ATP to ADP. Hsp40 family members contain a highly conserved J-domain that comes into contact with Hsp70 and stimulates its ATPase activity. Substrate release is later initiated by NEFs that bind Hsp70 and exchange ADP for a new ATP molecule, thus opening up Hsp70, releasing substrate, and resetting the cycle [20]. Human cytosolic NEF co-chaperones in the cytosol and ER lumen belong to one of three families: the Bcl1-associated athanogene (Bag) family, the Hsp110 family and the Hsp70 binding protein 1 (HSPBP1) family [27].

Cytosolic Hsp70 chaperones have a PTIEEVD motif at the extreme C-termini that is the binding site for tetratricopeptide repeat (TPR) domain co-chaperones [28]. One of these is HSP-organizing protein (HOP) that also contacts Hsp90 simultaneously. In some cases, the partially folded Hsp70-bound substrate is transferred via HOP complex formation to Hsp90, where further folding is encouraged until the native state is reached [29]. Another TPR-domain co-chaperone is the C-terminus Hsp70 interacting protein (CHIP) [30]. CHIP, which interacts with both Hsp70 and Hsp90, can ubiquitinate unfolded proteins bound by the chaperones, thus providing a link between the folding machinery and the degradative process [31, 32]. However, lumenal Hsp70 and Hsp90 (BiP/Grp78 and Grp94, respectively) do not have TPR-domain co-chaperones [33].

Hsp90 Family

Cytosolic Hsp90 functions downstream of Hsp70 and is not required for the *de novo* folding of substrates, but rather is essential for maturation and trafficking of particular proteins. Hsp90 has an N-terminal ATP-binding domain, a middle domain where substrates bind, and has a C-terminal homodimerization site [34]. Similar to Hsp70, Hsp90 also undergoes an ATPase cycle, where in the ATP-bound state Hsp90 has a high-affinity for substrate and after ATP hydrolysis the substrate is released [35, 36]. The cytosolic Hsp90 chaperones also contain an MEEVD motif at the extreme C-termini that is bound by TPR-domains, including HOP and CHIP [28]. Other TPR-domain co-chaperones are specific for Hsp90 including several peptidyl-prolyl *cis-trans* isomerases [37].

Figure 1.4: Hsp70 folding cycle

The Hsp70 cycle begins with Hsp70 in the ATP-bound state, which does not bind substrate. Hsp40 family co-chaperones (DNAJs) bind substrate, activate ATP hydrolysis and subsequent substrate binding to Hsp70. NEFs promote an exchange of ADP and rebinding of ATP, allowing for substrate release. In some cases, substrate is brought to Hsp90 through the Hsp-organizing protein (HOP) and folding of the substrate is completed. Alternatively, the substrate can get degraded if CHIP ligase interacts with Hsp70 to send substrate for degradation [17].

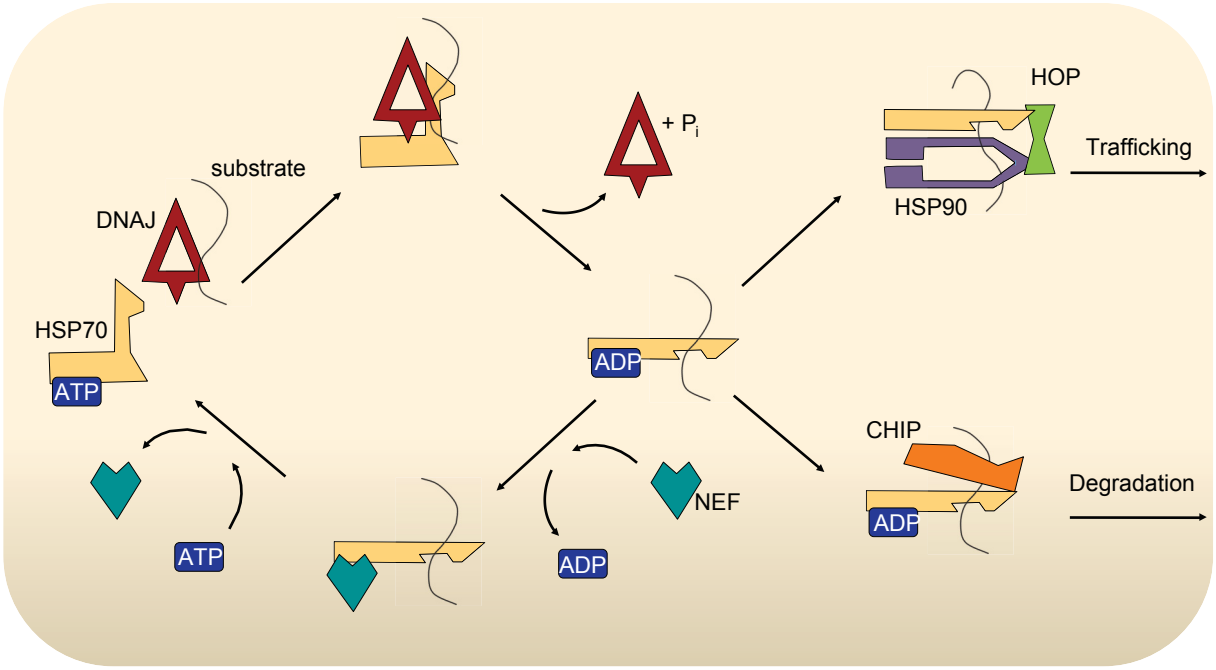
substrate
DNAJ
HSP70
ATP
+ P_i
ADP
HOP
HSP90
Trafficking
CHIP
ADP
Degradation
NEF
ADP
ATP

Degradation Machinery

ER Stress

Unfolded proteins will be recognized by chaperones and will re-enter the ATPase cycle until properly folded. Since unfolded or misfolded proteins can accumulate and cause cell stress, under certain conditions substrates will be removed rather than non-productively worked on by chaperones. If the protein folding process is disturbed or deemed unsuccessful, the substrate of interest will be put through a degradation process as a means to maintain cell homeostasis. ER stress can be stimulated by the disruption of protein folding and can further activate a process known as the unfolded protein response (UPR).

Unfolded Protein Response

For the cell to respond to ER stress and restore the ER to its normal physiological state, the cell will increase substrate folding mechanisms, clear unfolded proteins from the ER, and down regulate protein synthesis at both transcriptional and translational levels [38]. The UPR is induced by the downstream effects of three transmembrane proteins: inositol requiring 1 (IRE1), double-stranded RNA-activated protein kinase (PKR)-like endoplasmic reticulum kinase (PERK), and activating transcription factor 6 (ATF6) (Figure 1.5) [39]. The luminal domains of IRE1 and PERK normally associate with BiP, the Hsp70 in the ER lumen. Upon ER stress, BiP is recruited to aid in protein folding and as a result, IRE1 and PERK domains are free to oligomerize, activating UPR. IRE1 up-regulates ER chaperones and ER-associated degradation (ERAD) members through activation of the XBP-1 transcription factor, whereas PERK shuts off general

translation and up-regulates antioxidant elements. The third UPR transmembrane protein, ATF6, contains two Golgi localization sequences, and one of them is normally bound by BiP. Again, when BiP is competed away, the localization sequences are exposed and ATF6 is translocated to the Golgi where it is activated by proteolytic cleavage [40]. ATF6 is responsible for up-regulating BiP, XBP-1 and CHOP, among other targets, to induce UPR.

Figure 1.5: Unfolded Protein Response

ER stress involves the activation of three major stress sensors: protein kinase RNA-like ER kinase (PERK), inositol-requiring enzyme 1α (IRE1α), and activating transcription factor 6 (ATF6). Image modified from [41].

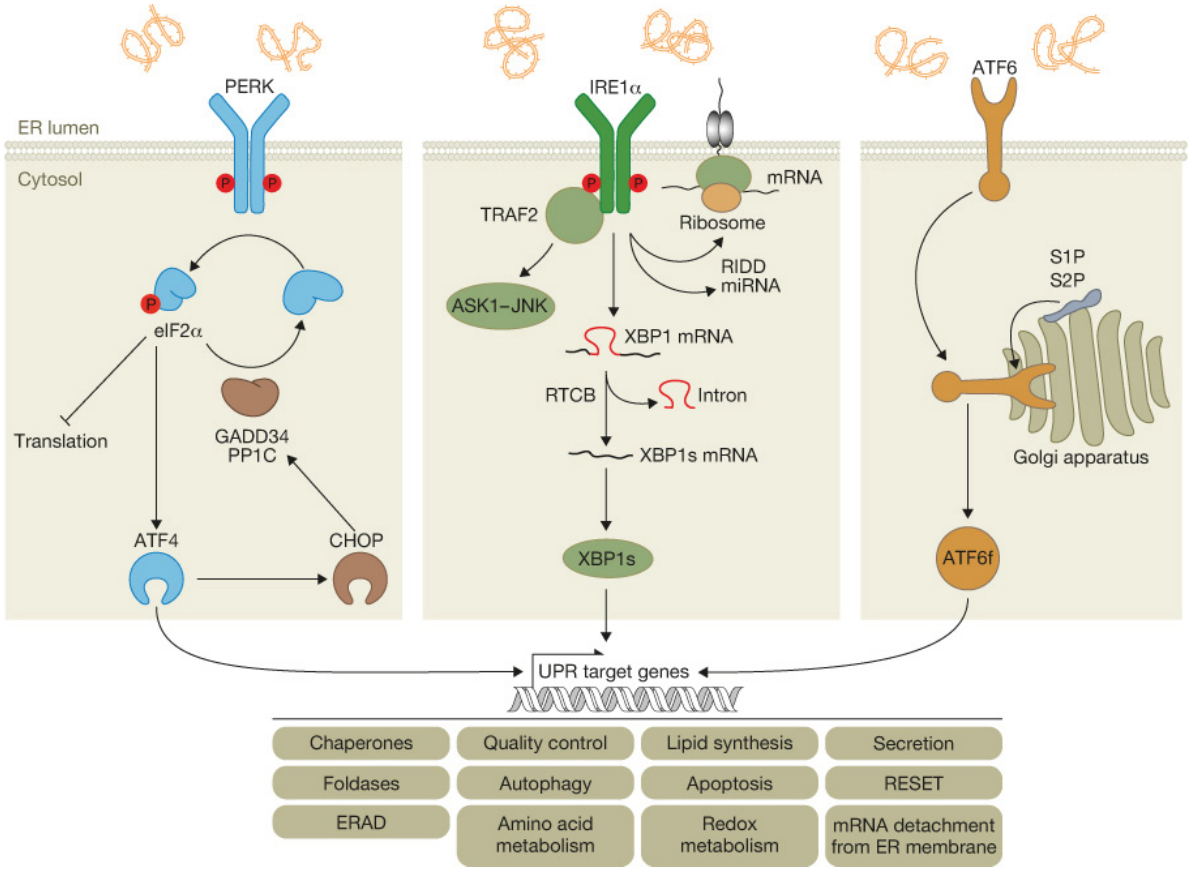
PERK
ER lumen
Cytosol
P
eIF2α
Translation
GADD34
PP1C
ATF4
CHOP
IRE1α
mRNA
TRAF2
Ribosome
RIDD
miRNA
ASK1–JNK
XBP1 mRNA
RTCB
Intron
XBP1s mRNA
XBP1s
ATF6
S1P
S2P
Golgi apparatus
ATF6f
UPR target genes
Chaperones
Quality control
Lipid synthesis
Secretion
Foldases
Autophagy
Apoptosis
RESET
ERAD
Amino acid metabolism
Redox metabolism
mRNA detachment from ER membrane

ER-Associated Degradation

Degradation of proteins can be induced during UPR, but the degradation of ER proteins is also a notable cell regulatory mechanism under normal growth conditions. Secretory proteins must be correctly folded before they exit the ER, but the extended interaction of misfolded proteins with ER or cytosolic chaperones can shift the fate of a protein to degradation if the protein is retained in the non-native state. If protein folding repair mechanisms by chaperones are unsuccessful, a process called ERAD takes place. Furthermore, ERAD can be used as a regulatory mechanism to manipulate the expression of proteins responsible for cellular processes, which will be discussed in more detail later on.

The ERAD process involves three primary steps where (1) misfolded proteins are recognized and targeted for degradation by polyubiquitination, (2) substrates are retro-translocated to the cytosol, and lastly (3) substrates are targeted for 26S proteasomal degradation (Figure 1.6) [42]. Each step of this process involves a complex of proteins of various members that interchange depending on the type of substrate that is entering ERAD.

Substrate Targeting

The maintenance of ER homeostasis is an essential process to the livelihood of the cell, but the mechanism by which substrates are targeted for ERAD is still not fully understood. In addition to substrate specific factors such as stability and folding rate, it is proposed that the environment of the ER also has heavy influence on how the cell distinguishes substrates for degradation. Some changes in the ER environment may

include fluctuations in Ca^{2+} levels, disruption of redox homeostasis, or infection of pathogens. ERAD substrate selection is largely completed by ER chaperones, where misfolded or prolonged chaperone-interacting proteins are targeted. In addition to chaperone identification of hydrophobic residues, the glycosylation state of the protein also determines its chaperone binding affinity.

N-Linked Glycoprotein Recognition

Most proteins that navigate through the secretory pathway display N-linked glycans, which are crucial for the recruitment of substrate folding factors that maintain ER homeostasis. The presence of a correct N-linked glycan indicates a properly folded protein whereas the processing of this moiety can suggest a less stable state, one which requires further folding. Oligosaccharyltransferases (OST) attach N-linked glycans to the asparagine of the folding substrate, then glucosidase I (GLsI) removes the terminal glucose residue. Glucosidase II (GlsII) removes another glucose residue, and now the monoglucosylated substrate can bind to ER lumenal chaperones calnexin (CNX) and calreticulin (CRT). These chaperones work to prevent aggregation, recruit the thioredoxin-family chaperone ERp57, and retain non-native substrate in the ER for proper folding [33]. GlsII will eventually remove the last glucose residue. If a non-native structure is still present after trimming of the three glucose residues and final release from calnexin, UDP-glucose: glycoprotein glucosyltransferase 1 (UGT1) will transfer a glucose molecule back onto the protein and therefore reinitiate the calnexin folding cycle. On the other hand, if a protein is terminally misfolded, it must be removed from CNX/CRT, which is completed by ER degradation-enhancing α-mannosidase-like protein

(EDEM) [43]. Trimming mannose moieties from substrates prevents re-addition of glucose and calnexin binding, and this form of the glycan can be recognized by lectin receptors OS-9 and XTP3-B that direct the substrates to degradation by E3 ubiquitin ligase complexes [44].

Non-Glycosylated Protein Recognition

Non-glycosylated proteins are largely recognized by molecular chaperones such as BiP in the lumen and Hsp70 in the cytosol. Co-chaperones also play a crucial role in steering the unfolded substrate to degradation, which is mostly seen with Hsp40 family proteins. It is proposed that the retention of substrate by the chaperone system indicates a heavily misfolded substrate and as such it is sent for degradation. BiP is thought to interact directly with E3 ubiquitin ligases in the ER membrane [45].

Ubiquitination: E1, E2, E3

After recognition of a misfolded protein for ERAD, a small (7.6 kDa) peptide ubiquitin must be added to the substrate so that it can be identified by the proteasome for degradation [46]. The ubiquitination process depends on three enzymes: E1, E2 and E3. The E1 ubiquitin-activating enzyme binds ATP, promoting a conformation where E1 forms a high-energy covalent bond with ubiquitin. As such, the E1 efficiently activates ubiquitin for subsequent steps involved in substrate degradation [47]. E1 adds ubiquitin to an E2 ubiquitin conjugating (UBC/UBE2) enzyme where ubiquitin is ready to be transferred to the substrate. Lastly, the E3 ligase provides specificity of the ubiquitination reaction, and will activate the transfer of ubiquitin from E2 to the substrate, and in some

cases will promote formation of polyubiquitinated chains linked through Lys-48 and the C-terminus of each ubiquitin [48]. The ubiquitination cycle is repeated to build up a polyubiquitin chain on the substrate, which is recognized by the proteasome, leading to the degradation of the ubiquitin labeled protein (Figure 1.6).

The ERAD complex is typically composed of one or more E3 ligases, among other proteins to aid in retro-translocation of the substrate. There are two families of E3 ligases: HECT domain E3s and RING E3s. In yeast, there are only two E3 ligases that make up ERAD complexes: Doa10p and Hrd1p [42]. In mammals however, there are several identified E3 ligases that make up ERAD complexes (Figure 1.7).

Figure 1.6: The Ubiquitin-Proteasome System (UPS)

First, ubiquitin-activating enzyme (E1) hydrolyzes ATP to form linkage with ubiquitin, which is then transferred to the ubiquitin-conjugating enzyme (E2). E2 enzymes work with E3 ubiquitin ligases to transfer the ubiquitin to the substrate. The polyubiquitinated substrate is then recognized by the 26S proteasome, which digests the protein substrate.

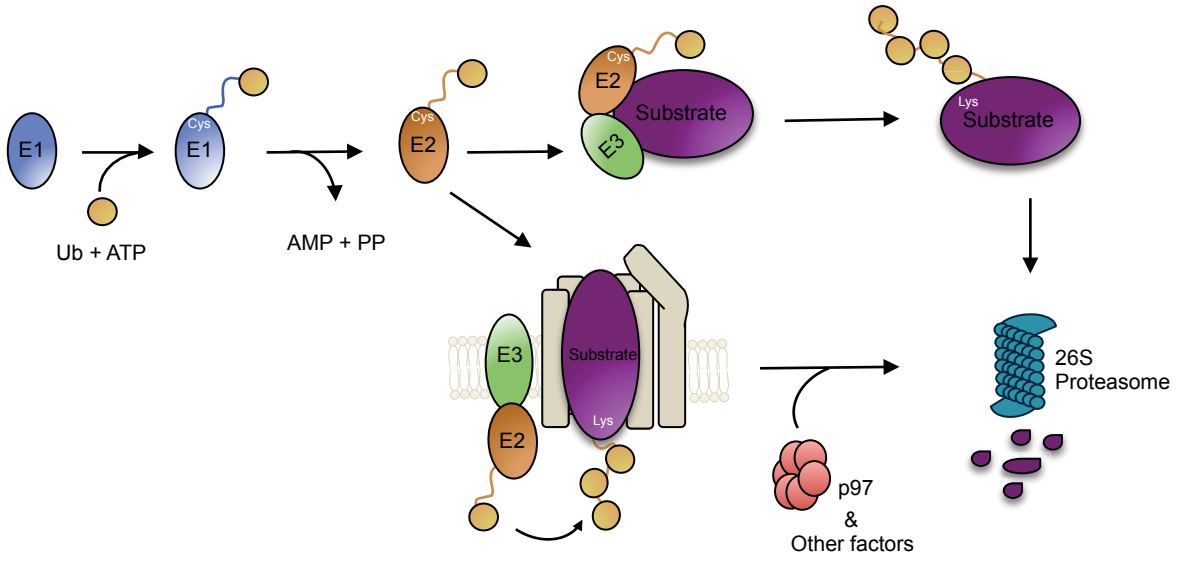
E1
Cys
E1
Ub + ATP
AMP + PP
Cys
E2
Cys
E2
Substrate
E3
Lys
Substrate
E3
Substrate
Lys
E2
p97
&
Other factors
26S
Proteasome

Figure 1.7: Mammalian ERAD complexes

The regulation of substrate degradation involves a complex system consisting of E2 conjugating enzymes, partnering E3 ubiquitin ligases, translocation machinery, and substrate removal cofactors. Depicted here are some well-studied ligases and ligase complexes, including HRD1, RMA1, gp78, TEB4 complexes and cytosolic CHIP and Parkin ligases. Obtained from [49].

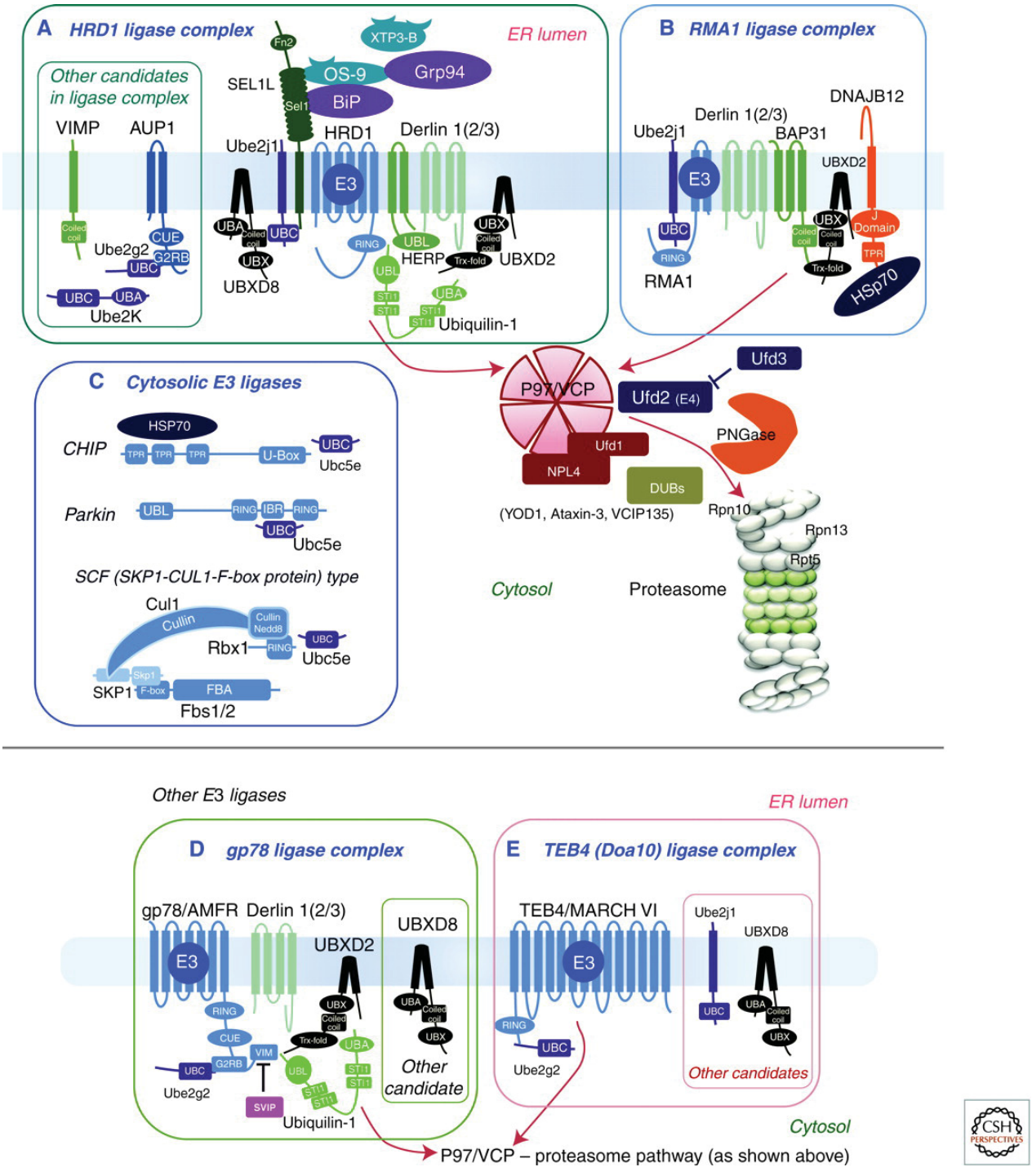
A HRD1 ligase complex
ER lumen
Other candidates in ligase complex
VIMP
AUP1
Coiled coil
Ube2g2
CUE
G2RB
UBC
UBC
UBA
Ube2K
Fn2
XTP3-B
SEL1L
OS-9
Grp94
Sel1
BiP
Ube2j1
HRD1
Derlin 1(2/3)
E3
UBA
Coiled coil
UBC
UBXD8
UBX
RING
UBL
HERP
Trx-fold
UBXD2
UBX
Coiled coil
UBL
ST1
ST1
UBA
ST1
ST1
Ubiquilin-1
B RMA1 ligase complex
DNAJB12
Derlin 1(2/3)
Ube2j1
BAP31
UBXD2
E3
UBC
RING
RMA1
UBX
Coiled coil
Coiled coil
Trx-fold
J Domain
TPR
HSp70
C Cytosolic E3 ligases
HSP70
CHIP
TPR
TPR
TPR
U-Box
UBC
Ubc5e
Parkin
UBL
RING
IBR
RING
UBC
Ubc5e
SCF (SKP1-CUL1-F-box protein) type
Cul1
Cullin
Cullin Nedd8
Rbx1
RING
UBC
Ubc5e
Skp1
SKP1
F-box
FBA
Fbs1/2
P97/VCP
Ufd2 (E4)
Ufd3
PNGase
Ufd1
NPL4
DUBs
(YOD1, Ataxin-3, VCIP135)
Rpn10
Rpn13
Rpt5
Cytosol
Proteasome
Other E3 ligases
ER lumen
D gp78 ligase complex
gp78/AMFR
Derlin 1(2/3)
UBXD8
UBXD2
E3
RING
CUE
VIM
UBC
G2RB
Ube2g2
UBX
Coiled coil
Trx-fold
UBA
UBL
ST1
ST1
ST1
ST1
SVIP
Ubiquilin-1
Other candidate
E TEB4 (Doa10) ligase complex
TEB4/MARCH VI
E3
RING
UBC
Ube2g2
Ube2j1
UBXD8
UBC
UBA
Coiled coil
UBX
Other candidates
Cytosol
P97/VCP – proteasome pathway (as shown above)

Retro-Translocation

The degradation machinery, namely the 26S proteasome, is located in the cytosol rather than the ER lumen where the protein substrates are held. Blocking retro-translocation induces ER stress and UPR, so it is essential that the substrate be transported across the ER membrane in order to complete the degradation process. The machinery for protein ubiquitination spans the ER membrane and works in tandem with additional proteins so that the substrate can be transported across the ER into the cytosol. Upon transfer to the cytosol, the 26S proteasome de-ubiquitinates the substrate as it degrades the protein.

Identified Members Of The Translocon

It seems reasonable that mammals have more highly diverse ERAD complexes than yeast due to the variety of ER-bound E3 ligases. There is still much to discover about the ERAD processes in mammals, but the variety in ligases must contribute to the efficiency of substrate-specific recognition, retrotranslocation, ubiquitination, and proteasomal degradation. In addition, some of the reoccurring ERAD complex members have been identified (Figure 1.7).

In yeast, the Doa10p E3 ligase degrades transmembrane proteins with cytosolic domains whereas Hrd1p forms a large complex to degrade transmembrane and lumenal proteins. In mammalian cells, the variety of ligases is much greater. In addition to ER-bound homologues of Hrd1p: HRD1 and Gp78, and homologue of Doa10p: TEB4, mammals also have other ER-bound E3 ligases RMA1, TRC8, RNF170 and TMEM129 and a cytosolic E3 ligase CHIP [50]. The two most common RING ubiquitin ligase

systems are HRD1 and gp78, both which are bound to the ER and degrade the majority of misfolded ERAD substrates. HRD1 and gp78 contain multiple transmembrane helices, consistent with them forming at least part of a retro-translocation pore. Thus, polyubiquitination can be coordinated with removal from the ER membrane [51]. TRC8 also has multiple transmembrane helixes, but their role is not yet clear. The identification of ERAD E3 ligases must be completed on a substrate-by-substrate basis, and although the retro-translocon members vary for each substrate, the process and certain common ERAD components remain the same.

Either subsequently or simultaneously with ubiquitination, the substrate is removed from the ER with the assistance of ERAD members such as ER resident rhomboid-like pseudo-protease Derlin-1, -2 or -3, and UBXD8, which help recruit ATPase valosin-containing protein (p97) and its cofactors ubiquitin fusion degradation 1 (Ufd1) and nuclear protein localization 4 (Npl4) to the ERAD complex. The energy from cytosolic AAA-family ATPase p97 drives the protein extraction, thus completing translocation from the ER. Not all substrates rely on p97 for ER removal, and retro-translocation of ER bound proteins can be completed independently, even though p97 is required for normal ER function [52].

In one example of clinical interest, the ER is crucial for the formation and transport of major histocompatibility complex (MHC) class I and II molecules and also regulates the secretion of immune mediators [53]. Like other secretory proteins, MHC-I molecules must pass through the ER to the Golgi and ultimately be presented at the cell surface in order to initiate an immune response. Some pathogens evade the human cell immune response by preventing MCH-I presentation, such as by manipulating ERAD to

degrade MHC-I molecules and preventing substrate trafficking. Notable research on the human cytomegalovirus (HCMV) shows that viral proteins US2 and US11 are expressed early in infection and send MHC-I molecules for cytosolic degradation [54]. Derlin1 aids the retro-translocation of MHC-I across the ER membrane, and gp78, TRC8, and signal peptide peptidase (SPP) make up the ERAD complex to help degrade MHC-I molecules when initiated by US2 HCMV protein [50, 55].

In another well-studied example, mutations in the cystic fibrosis transmembrane conductance regulator (CFTR) chloride/bicarbonate channel cause its misfolding, ERAD and loss of function, leading to cystic fibrosis. One CFTR mutation, ΔF508, is responsible for the majority of cystic fibrosis cases. CFTR-ΔF508 is recognized by multiple E3 ligases at the ER: gp78 in complex with RMA1, and CHIP in complex with Hsp70. RMA1 may act even during translation of CFTR, whereas CHIP acts post-translationally, so that the different E3 ligases recognized separate misfolded states[56-58].

Other Functions Of ERAD

In addition to degrading misfolded proteins, ERAD also seems to play a regulatory role that impacts the physiological function of the cell. Some examples worth discussing include the turnover of ER membrane-bound proteins such as activated IP_3 receptor, HMG-CoA reductase (HMG-CoAR), and heme oxygenase-1 (HO-1).

Calcium IP_3

The ER serves as an intracellular source of calcium and inositol 1,4,5-triphosphate (IP_3) receptors control the Ca^{2+} release upon activation. IP_3 ion channel activation is important for increasing calcium levels for signaling pathways, gene expression, and apoptosis [59]. Since IP_3 channels are degraded by ERAD, which would lower the cytosolic amount of calcium, it seems that ERAD can be associated with regulating Ca^{2+} induced signaling pathways, and therefore have an influential role in the prevention of apoptosis.

Sterols

In order to prevent the overproduction of cholesterol, cells have developed sterol-regulated ubiquitination of 3-hydroxy-3-methylglutaryl coenzyme A reductase (HMG CoAR). HMG-CoAR is responsible for catalyzing the rate-limiting step in cholesterol synthesis. Its regulation involves sterol-induced binding of HMG-CoAR with ER bound INSIG-1 and INSIG-2 proteins, which are associated with ERAD machinery such as E3 ligase gp78 and TRC8 [60] [61]. In this way, ERAD machinery has an influential role on lowering plasma cholesterol levels.

Heme catabolism

Heme oxygenase-1 (HO-1) catalyzes the rate-limiting step in the degradation of heme to produce biliverdin, iron and carbon monoxide. HO-1 expression is induced by oxidative stress and it plays a role in preventing inflammation and apoptosis [62]. HO-1 is highly expressed in cancer cells due to its antioxidant activity but is shown to be

degraded by an ERAD complex that contains E3 ligase TRC8 [63]. ERAD of HO-1 also requires its cleavage in the transmembrane domain by SPP [64]. Understanding ERAD can bring a greater understanding to cell oxidation mechanisms, and could even provide a means to target cancers.

The functions of ERAD go beyond folding proteins and include mediating a variety of cellular mechanisms by influencing calcium concentration, sterol production, and oxidative state. As such, an enhanced understanding of ERAD complexes and subsequent degradation pathways can elucidate both substrate degradation fate as well as the physiological state of the cell.

hERG Specific Folding and Degradation

The protein folding process and its associated QC mechanism embody a fundamental component of the secretory pathway. As such, failure to maintain these processes has heavy implications for generating human disease. Neurodegenerative disorders such as Parkinson's disease and Alzheimer's can result from the inability to clear misfolded aggregated proteins [65]. On the other hand, ion-channel misfolding diseases such as cystic fibrosis (CF) or long QT syndrome (LQTS) present defective folding and/or trafficking of the channel to the cell surface, thus presenting loss of function [17]. Unlike CF, which is a recessive disorder and has a common clinically presented mutation (ΔF508), LQT2 is dominantly inherited and has hundreds of mutations causing disease. In order to understand how the misfolded hERG protein causes LQT2, the folding and degradative pathways that it undergoes must be examined.

Our lab and others previously identified that hERG folding was dependent on Hsp90 [66], Hsp70, and the Hsp40 co-chaperone DNAJA1, but overexpression of DNAJA1, DNAJA2 and DNAJA4 also promoted hERG ERAD [67]. In both mouse cardiac myocytes and human cells, over-expressing Hsp90 increased an FG band of ERG, while CHIP ligase over-expression decreased both CG and FG forms, indicating a conserved mechanism where CHIP degrades hERG and Hsp90 promotes folding and trafficking [67, 68]. Overexpressed Hsp70 was reported to promote hERG folding and Hsc70 to promote degradation by CHIP [69] but we were not able to observe this in our own experiments (Christine Hantouche, unpublished). The cytosolic RING domain E3 ligase RNF207 was found to enhance hERG expression instead of degrading it, by an unknown mechanism [70].

The impact of Hsp40 proteins in Hsp70-induced folding is seemingly specific to the type of DNAJ protein and substrate involved, but it is suggested that that the co-chaperones involved in the folding cycle are maintained at optimal levels [67]. In more recent work, our lab identified another co-chaperone of Hsp70, NEF Bag1, that promotes Hsp70 and CHIP removal from hERG complex, promoting the degradation of a potentially more heavily misfolded state (Christine Hantouche, Doctoral Thesis). Furthermore, we have identified the E2 conjugating enzyme, Ube2g2, and its partnering E3 ligase TRC8, as ERAD proteins that promote hERG degradation even without NEF manipulation (Christine Hantouche, Doctoral Thesis). There is little research elucidating the nature of ERAD E3 ligases that are involved in hERG degradation, but we believe that we have identified a new pathway for misfolded hERG degradation, relevant to misfolding mutations in LQT2.

TRC8 Substrates

Relatively little is known about TRC8 ERAD mechanisms or what partnering proteins work with TRC8 in an ERAD setting, but this would seemingly be the first time that TRC8 is implicated as having a role in protein quality control. It is not clear whether any of the known TRC8 substrates are misfolded proteins, although the role of TRC8 at the ER has been implicated in relieving ER stress. The identified substrates that TRC8 sends for degradation are important for cell stress mechanisms, in response to pathogens and ER stress, and for regulation of sterols.

Sterol regulation

TRC8 is implicated in disorders associated with ER stress, and in particular is thought to progress non-alcoholic fatty liver disease (NAFLD) since TRC8 is down-regulated in steatotic livers [71]. More evidence for the role of TRC8 in lipogenesis and cholesterol synthesis is displayed by its regulation of sterol regulatory element-binding proteins (SREBPs) trafficking [72] as well as with its degradation of HMG-CoAR [61]. Proteins such as SREBPs, HMG-CoAR, and TRC8 all possess a sterol-sensing domain and all regulate sterol synthesis. The presence of low cholesterol results in SREBP and SREBP cleavage-activated protein (SCAP) trafficking from the ER to the Golgi, where proteases cleave SREBP so it can transport to the nucleus to transcribe cholesterol and fatty acid-synthesis genes [73]. TRC8 however hinders the complex of SREBP-2 and SCAP, thus preventing SREBP-2 from transporting to the Golgi and becoming an activated transcription factor that up-regulates lipid genes such as HMG CoAR [74]; [75].

Furthermore, the presence of sterols can also prevent SREBP Golgi trafficking by permitting INSIG-1 to bind to SCAP, thus retaining SREBP at the ER and preventing

further sterol production [76]. TRC8 has another role in interfering with INSIG-1 and possibly INSIG-2 retention of SREBP:SCAP at the ER, and giving another mechanism by which TRC8 regulates lipid production [77]. Sterol-induced binding of INSIG-1 and INSIG-2 to HMG-CoAR results in the degradation of the reductase, where INSIG-1 mediates gp78 degradation and both INSIG-1 and INSIG-2 mediate TRC8 degradation of HMG-CoAR [61]. Furthermore, TRC8 is shown to mediate the degradation of INSIG1, providing more evidence of a functional role of the sterol sensing domain present in the N-terminus of TRC8 [61] [74].

TRC8 seems to play multifaceted role in the regulation of intracellular cholesterol production. More specific to cardiovascular disease is seen with the use of statins to lower the low-density lipoproteins (LDL)-cholesterol [78]. However, statins also inhibit sterol production that feedback on the regulation of HMG-CoAR. Diet induced sterol-accelerated degradation contributes to the regulation of HMG-CoAR in mice, and it may be possible that TRC8 could contribute to the cholesterol regulation in cardiovascular disease too [74].

Furthermore, TRC8 can inhibit sterol synthesis by degrading the SREBP:SCAP complex and by degrading HMG-CoAR, but may also regulate sterol production through degrading INSIG1, which allows SREBP to mature to a transcription factor and also allow HMG-CoAR to synthesize cholesterol. Additionally, the stability of TRC8 decreases under higher levels of sterols, although the effects are minimal [77] and TRC8 is also reported to self-ubiquitinate, further complicating the regulatory role that TRC8 has in sterol synthesis and any other regulation of its substrates [75].

Cell Stress/Infection

Of perhaps even more interest is TRC8s role in cell stress mechanisms, which will be discussed here. Firstly, under the induction of human cytomegalovirus (HCMV) US2 gene product, TRC8 works with Derlin-1 and the intramembranous protease signal peptide peptidase (SPP) to degrade major histocompatibility complex (MHC) class I heavy chain molecules, thus encouraging a developed viral infection by avoiding cellular detection and preventing a proper immune response [79, 80].

Another viral hijack of the TRC8 ERAD pathway is seen with the removal of the hepatitis C virus (HCV) immature core protein from the ER, allowing a mature core protein to propagate the viral infection, which is associated with liver disease [81]. The cleavage of HCV core protein to the mature form is completed by SPP and TRC8 degrades incompletely processed immature core protein. Accumulation of the immature form causes ER stress, and clearance by TRC8 may be seen as an attempt to alleviate the cells of ER stress and properly reform the ER structure [81]. This mechanism advances HCV infection however, since the processing of the core protein allows for its maturation, producing infectious HCV particles and progressing the infection [81].

Lastly, TRC8 plays a more regulatory role in degrading the unfolded protein response (UPR) regulator XBP1u [82]. In the UPR, IRE1 is activated where it splices XBP1 pre-mRNA encoding inactive XBP1u, to the final form encoding active XBP1s transcription factor, which will subsequently turn on UPR genes. XBP1s negatively regulates UPR by targeting XBP1u for degradation through SPP, Derlin1 and TRC8 [82]. XBP1u is localized at the ER and similar to other single transmembrane spanning substrates of TRC8, relies on SPP [83]. In the cell model of HCV infection mentioned

above, knocking out both SPP and TRC8 resulted in an accumulation of HCV immature core protein in the ER, inducing ER expansion and activation of UPR by regulating the spliced variant XBP1s [81]. TRC8 certainly has a role in the regulation of UPR during cellular stress, and we propose that TRC8 degrades a misfolded and potentially stress-inducing form of hERG.

Objectives and Rationale

Of the hundreds of mutation that cause LQT2, many of them cause misfolding of hERG protein at the ER, followed by inhibited trafficking to the cell surface or impaired function. Our lab previously identified Hsp70 co-chaperone NEF, Bag1, to promote the ERAD pathway of hERG (Christine Hantouche, Doctoral Thesis). In this scheme, Bag1 dissociated Hsp70 from hERG, and as such prevented a properly folded protein state from forming. Of particular interest, Bag1 also inhibited the cytosolic E3 ligase, CHIP from maintaining its complex with hERG. Since CHIP is the only known E3 ligase to degrade hERG at the ER, it was of interest to find what E3 is responsible for degradation of misfolded hERG. To this end, a siRNA screen was done to identify the E2 enzyme Ube2g2, and its partnering E3 ligase, TRC8, to degrade hERG. This is a novel role for Bag1 in shifting the degradation of hERG away from the action of CHIP and towards other E3 ligases. Here, we hope to elucidate the role of TRC8 in degradation of misfolded hERG substrate and further identify other partnering ERAD complex members that are involved in the degradation of this misfolded form of hERG.

Chapter 2

Results

TRC8 degrades hERG

We conducted an initial siRNA screen to find ER-anchored E3 ubiquitin ligases involved in the degradation of hERG. In HeLa cells stably expressing hERG (hERG1a), we detected the two forms of hERG by Western blot: an immature, ER form represented as a 135 kDa core-glycosylated (CG) band, and a mature 155 kDa fully glycosylated (FG) band that has successfully trafficked through the Golgi apparatus. The results identified TRC8 to restore hERG levels when the cells were exposed to TRC8 knockdown (Figure 2.1B). The increase in hERG was greatest for the CG form, around 20% above the control. Furthermore, the other E3 ligases tested by knockdown – TEB4, RMA1, HRD1 and gp78 – did not have an effect on the CG or FG forms of hERG.

Subsequently, we investigated the role of TRC8 on the degradation of hERG by co-expressing TRC8 constructs with WT-hERG plasmid. To examine the effect of TRC8 we included two ubiquitin-inactive TRC8 mutants as controls. The TRC8 constructs included a wild-type TRC8 form, a RING mutant construct and a truncated form that lacks the RING domain, ΔRING (Figure 2.1A). The RING mutant has two point mutations at position 447 and 450, which are mutated from cysteine to alanine and lose their role of ubiquitination and their interaction with the E2 enzyme [84]. For these

experiments, we adjusted the amounts of the TRC8 constructs to have similar levels of expression so that we could compare the effect on hERG.

HEK293 cells were used for co-expression experiments as previously established, and hERG was again detected by Western blot [Walker 2010]. TRC8 co-expression with WT-hERG decreases the total amount of CG and FG hERG to ~50% and 55%, respectively, when compared to empty vector control (Figure 2.1C). While the expression of hERG in the presence of ΔRING was similar to control, the RING mutant resulted in less FG form of hERG, but normal amounts of CG hERG (Figure 2.1C).

Since TRC8 is an ER-localized E3 ligase and the RING domain was important for its effect, it seemed reasonable to speculate that TRC8 was sending hERG for ERAD, thus resulting in less hERG that could traffic and mature to the Golgi and beyond. To examine the kinetics of hERG trafficking, we performed pulse chase experiments in HEK293 cells co-expressing hERG, WT-TRC8 and ΔRING. Over a 6 h time course, the amount of CG hERG decreased to ~70% compared to the starting amount of total hERG in control cells, and the subsequent FG amount matured to ~30% (Figure 2.2A). In our internal control, the ΔRING expressing cells showed a decrease in CG hERG to ~52% after 6 hours, whereas the FG amount matured similarly to control cells to ~30% (Figure 2.2A). When TRC8 was co-expressed with hERG, the CG hERG decreased to ~31% compared to the starting pool of hERG, and the subsequent amount of FG hERG was reduced to ~16%, close to half of the controls (Figure 2.2A). We also looked at the trafficking of hERG in cells expressing the RING mutant and found that, similar to steady state results, the CG form of hERG was comparable to the control, where as FG hERG appeared at a rate similar to that with TRC8 (Figure 2.2B). The reduction in hERG

under TRC8 co-expression was due to the degradation of hERG at the ER, which is likely going through ERAD.

Figure 2.1: The E3 ligase TRC8 degrades hERG at the ER

A, Diagram of TRC8 constructs used for plasmid transfections. Transmembrane domains are numbered and the RING domain is labeled. The loss of ubiquitination activity due to C547A and C550A mutations are shown in RING-mut with a star. Right panel shows TRC8 protein structure. B, HeLa cells stably expressing WT-hERG were transfected with siRNA against the indicated E3 ligase, or non-silencing control. The reduction of ligase proteins and the expression of CG and FG hERG were analyzed by immunoblot 48 hours after transfection. Sample lysate protein concentration was measured using the DC Protein Assay Kit (BioRad) and were normalized with lysis buffer. Expression of hERG was quantified relative to the amount in control cells (TRC8, n=7; TEB4, n=8; RMA1, n=6; HRD1 and gp78, n=5). C, HEK293 cells were transiently transfected with HA tagged hERG and the indicated TRC8 construct or vector control. 48 hours after transfection, the expression of CG and FG hERG was detected by immunoblot and quantified as above (n=3). Bands corresponding to full-length TRC8 and TRC8-ΔRING are marked.

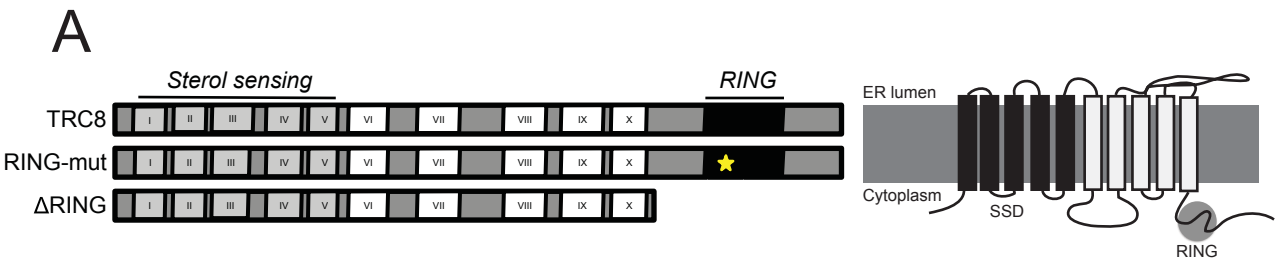
A
Sterol sensing
RING
TRC8
RING-mut
ΔRING
I
II
III
IV
V
VI
VII
VIII
IX
X
ER lumen
Cytoplasm
SSD
RING

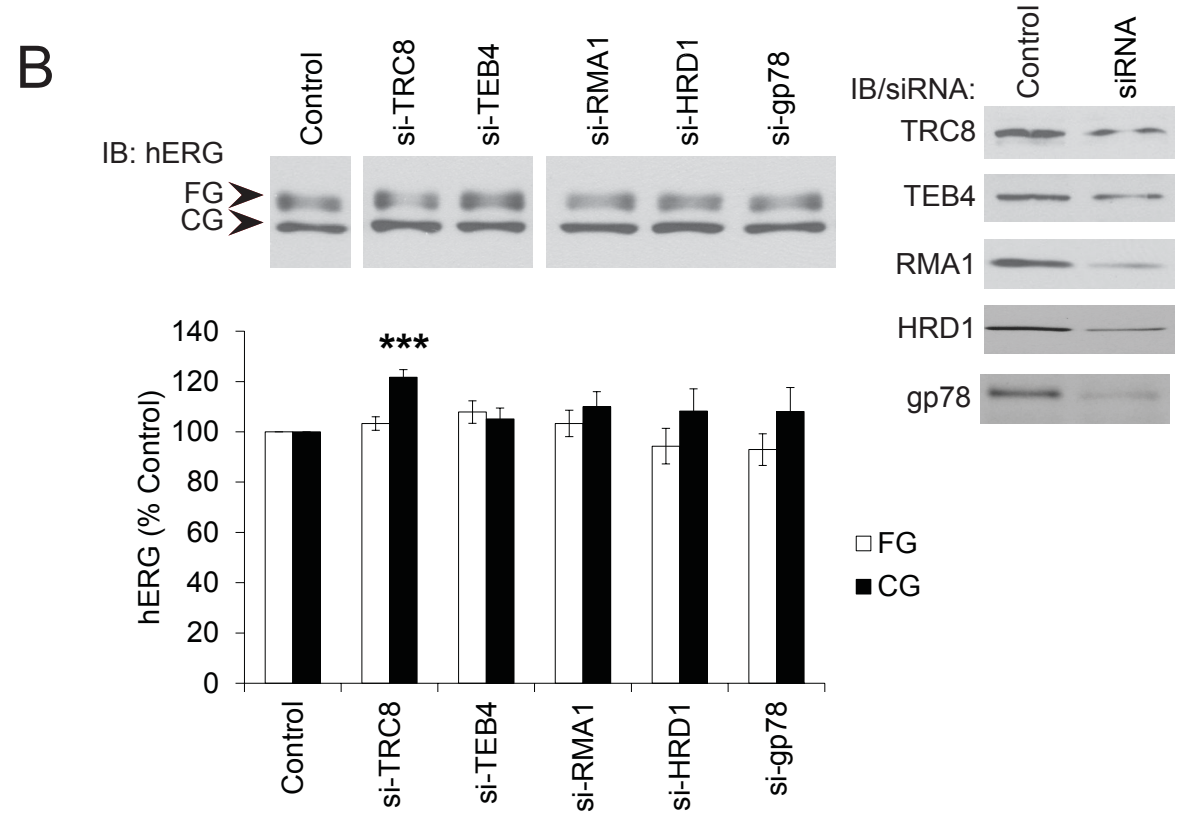
B
IB: hERG
FG
CG
Control
si-TRC8
si-TEB4
si-RMA1
si-HRD1
si-gp78
IB/siRNA:
Control
siRNA
TRC8
TEB4
RMA1
HRD1
gp78
hERG (% Control)
140
120
100
80
60
40
20
0
***
FG
CG

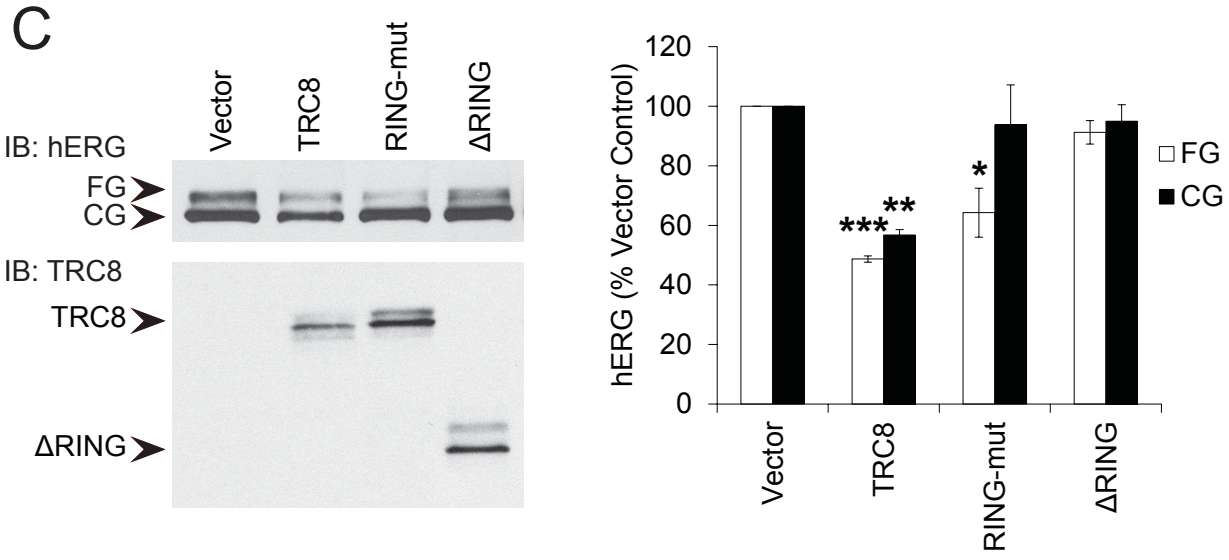
C
IB: hERG
FG
CG
IB: TRC8
TRC8
ΔRING
Vector
TRC8
RING-mut
ΔRING
hERG (% Vector Control)
120
100
80
60
40
20
0
***
**
*
FG
CG

Figure 2.2: TRC8 accelerates hERG degradation

A, HEK293 cells were transfected with hERG and the indicated TRC8 construct or vector control. 48 hours post transfection cells were radioactively labeled for one hour and chased for six hours. Cells were lysed every two hours, immunoprecipitated for hERG and the expression of CG and FG hERG was quantified relative to the amount in control cells at t=0. (Vector and TRC8, n=6; TRC8-ΔRING, n=3). B, Cells were transfected as in A, but with RING-mut (n=3).

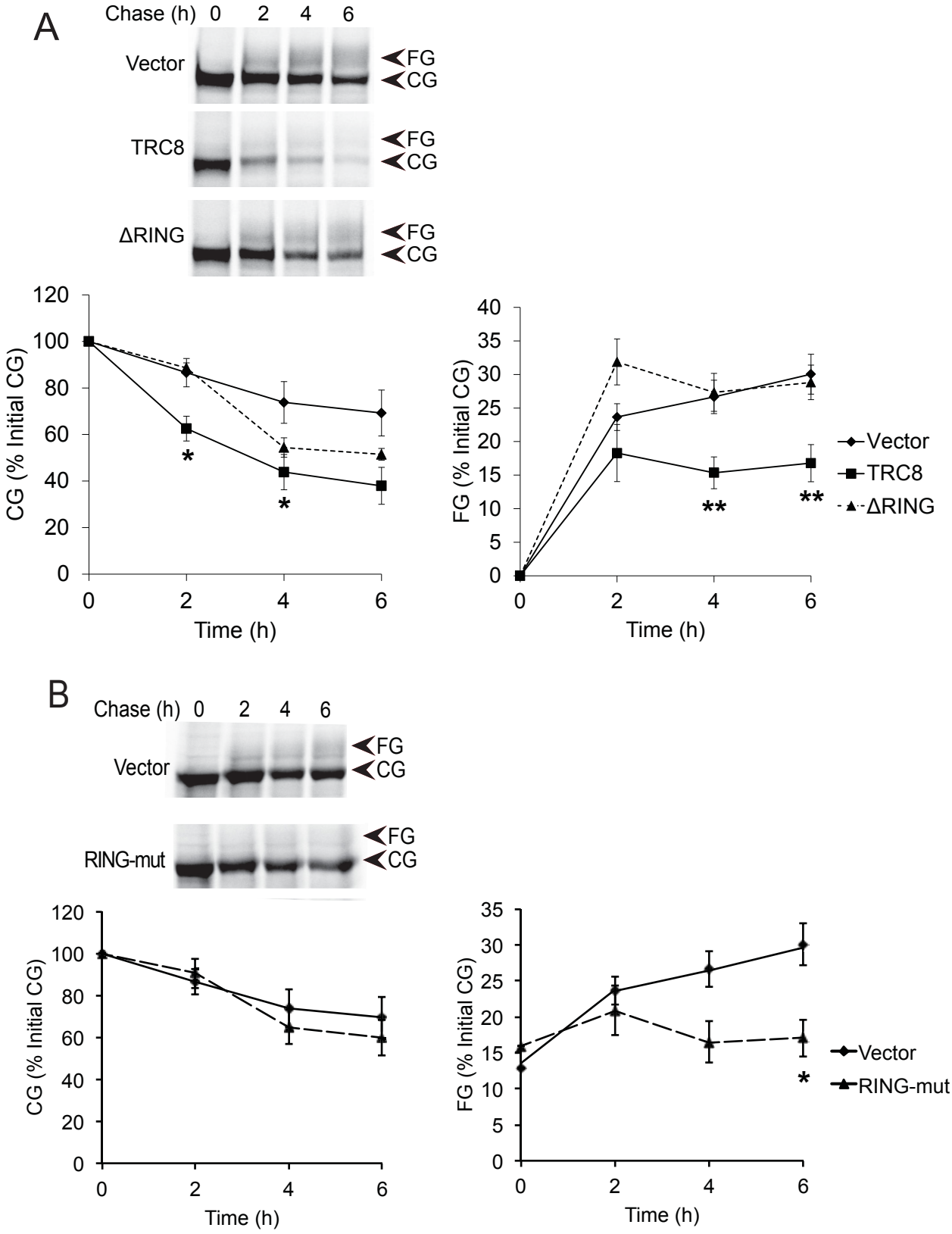
A
Chase (h) 0 2 4 6
Vector
TRC8
ΔRING
FG
CG
CG (% Initial CG)
Time (h)
FG (% Initial CG)
Vector
TRC8
ΔRING
B
RING-mut
CG (% Initial CG)
Time (h)
FG (% Initial CG)
Vector
RING-mut

TRC8 interacts and ubiquitinates hERG

To determine if TRC8 could in fact recognize hERG as a substrate to ubiquitinate and consequently degrade through ERAD, we proceeded to perform co-immunoprecipitations of hERG. In addition, we used the TRC8 mutants to ask which part of TRC8 was responsible for binding hERG. HEK293 cells were transfected with hERG and empty vector, TRC8, RING mutant or ΔRING constructs. We found that all three forms of TRC8 were detected in the samples with immunoprecipitated hERG (Figure 2.3A). We previously postulated that TRC8 degradation worked independently of the Hsp70 cycle, and indeed we find the expression of Hsp70 is unchanging under TRC8 construct expression in both the total cell lysate and in the immunoprecipitated hERG complexes (Figure 2.3A). These results suggested that the TRC8 transmembrane region is sufficient for interaction with hERG.

Since TRC8, RING mutant and ΔRING interact with hERG, we wanted to confirm the polyubiquitination activity of TRC8 on hERG. In subsequent hERG immunoprecipitations under conditions that preserved polyubiquitin chains, we detected polyubiquitin by Western blot and quantified the amount relative to the total amount of hERG. The results showed that TRC8 caused around a 3-fold increase in polyubiquitinated hERG compared to controls, whereas co-expression of hERG with RING mutant and ΔRING did not (Figure 2.3B).

TRC8 certainly decreases the total amount of hERG through ubiquitination and subsequent degradation, as shown by densitometry of Western blots. However, the FG band of hERG represents a form that has trafficked past the Golgi apparatus, but it does not necessarily represent a cell surface hERG ion channel. As such, the functional

amount of hERG at cell surface may be less than what we reported by Western blot. To test the effect of TRC8 on hERG function, we conducted patch clamp measurements of whole cell hERG currents in HEK293 cells. We found that co-expressing hERG with TRC8 reduced the functional amount of hERG as measured by tail current density to ~30% of vector control (Figure 2.3C). TRC8-induced degradation therefore lowers the protein expression and results in a reduction of the physiologically relevant hERG current at the cell surface.

Figure 2.3: TRC8 prevents trafficking of a functional form of hERG

A, HEK293 cells were transfected with the indicated HA-tagged TRC8 construct, and hERG immunoprecipitated (IP) after 48 hour transfection. Lysates are shown as an input reference and co-precipitating TRC8 is shown on the right after immunoblot using specific antibodies against TRC8 and the HA tag, and Hsp70 detected as a control. B, Similarly to A, cells were transfected and immunoprecipitated hERG ubiquitination amounts were plotted relative to the ubiquitin amount in the control. C, HEK293 cells were transfected with hERG, GFP and either TRC8 or vector control. Tail current density from patch clamp measurements as in Fig. 1D are shown (n=6).

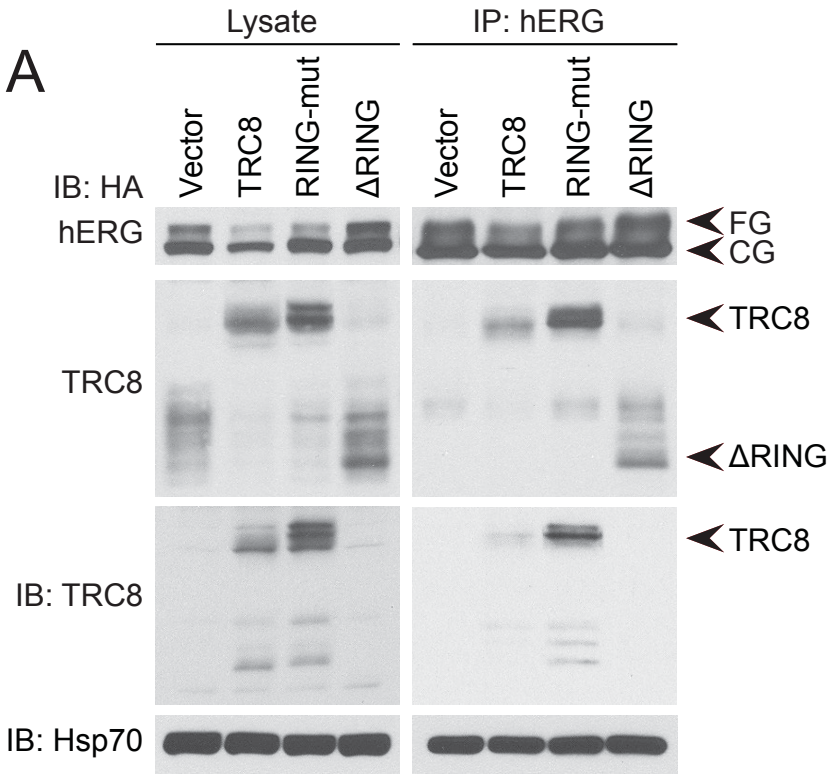
A
Lysate
IP: hERG
Vector
TRC8
RING-mut
ΔRING
IB: HA
hERG
FG
CG
TRC8
ΔRING
IB: TRC8
IB: Hsp70

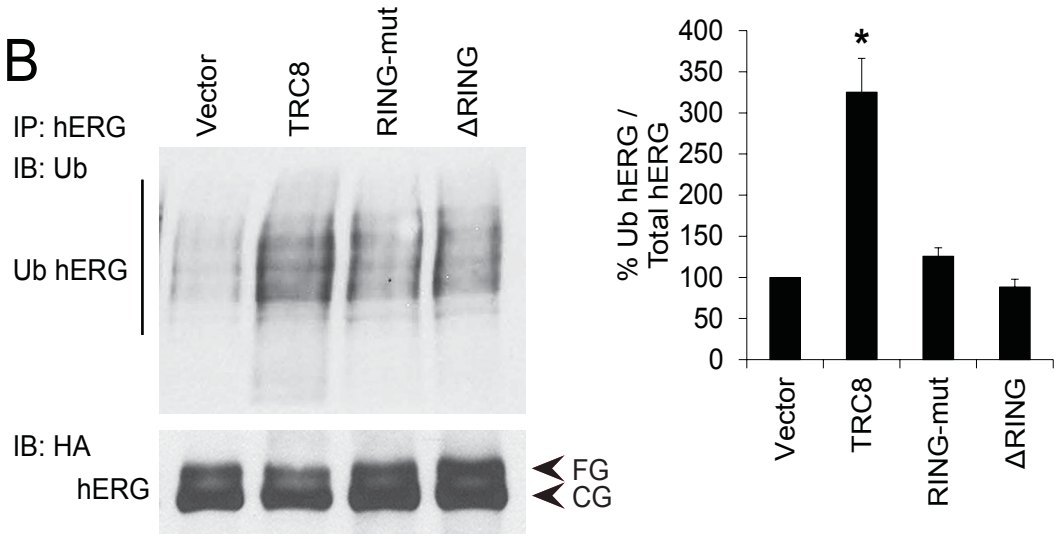
B
IP: hERG
IB: Ub
Ub hERG
IB: HA
hERG
Vector
TRC8
RING-mut
ΔRING
FG
CG
% Ub hERG / Total hERG
400
350
300
250
200
150
100
50
0
*

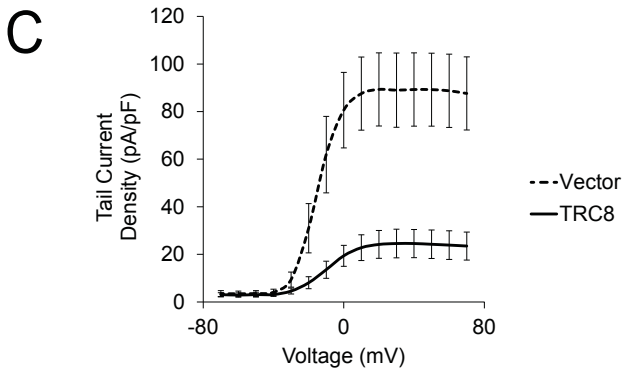
C
Tail Current Density (pA/pF)
120
100
80
60
40
20
0
-80
0
80
Voltage (mV)
Vector
TRC8

TRC8 degrades a misfolded form of hERG

Previously, our lab identified a novel pathway for the degradation of hERG at the ER. We formerly identified Bag1 as an NEF co-chaperone of Hsp70 that induced a more misfolded form of hERG, leading to more degradation. Now, our identification of TRC8 as an E3 ubiquitin ligase important for hERG degradation suggested that it recognizes misfolded or partially folded forms of hERG. We therefore wanted to examine if TRC8 degraded a misfolded mutant hERG in addition to the wild-type form of hERG. To address this, we used two HeLa cell lines that stably expressed either a pore mutant G601S hERG or F805C, which is mutated in the cytosolic cyclic nucleotide-binding domain. Both of these mutants were known to cause hERG retention and degradation in the ER, and G601S trafficking can be partially rescued by growth at 27°C, consistent with a folding defect [85-87]. Again, we used siRNA knockdown methods to lower the expression of Bag1, TRC8, and two other ER-bound E3 ligases HRD1 and gp78 to see if these played a role in mutant hERG degradation. When the cells were grown at the permissive temperature of 27°C, both Bag1 and TRC8 knock down increased the FG form of G601S hERG, whereas the other ER-bound E3 ligases did not have an effect (Figure 2.4A). The F805C hERG did not have a significant change in the CG form, and the FG form was negligible, so it was not quantified.

After identifying that G601S is degraded by TRC8, we proceeded to use a hERG pharmaceutical modulator, E-4031, that is thought to stabilize the channel. E-4031 is known to increase trafficking of G601S and some other hERG mutants but block its channel; the drug also stabilizes the structure of another misfolded hERG mutant, N470D [87, 88]. We wanted to determine if TRC8 still degraded mutant G601S hERG after

inducing a stable structure. In HEK293 cells, wild-type or G601S hERG was co-transfected with either empty vector or TRC8. Again, co-expression of TRC8 decreased the CG and FG forms in the wild-type hERG cells, but with E-4031 drug treatment, both CG and FG forms of hERG increased to be comparable to that in empty vector (Figure 2.5A). In the cells expressing mutant G601S, TRC8 co-transfection significantly lowered the CG form of G601S both with and without treatment, but in the E-4031 treated cells there was a significant increase in G601S hERG FG (Figure 2.5A). This indicates that TRC8 degrades a misfolded form of hERG in preference to a structurally stable form. Although E-4031 has been reported to be a structurally stabilizer of wild type and mutant forms of hERG [87-89], direct evidence for this stabilization of G601S was lacking. As such, we performed limited proteolysis of G601S hERG in light microsomes from cells that were grown in either normal media or in the presence of E-4031. In the absence of E-4031, the CG form was mostly degraded by 10 ng/mL trypsin (Figure 2.5B). Treatment with E-4031 produced a FG form as seen previously, which was also resistant to up to 10ng/mL of trypsin or more (Figure 2.5B). The CG form with E-4031 also showed more resistance at 10 ng/mL trypsin (Figure 2.5B). Thus, E-4031 structurally stabilizes G601S hERG, which seems to protect it from TRC8-mediated degradation.

Figure 2.4: TRC8 degrades misfolded mutant hERG-G601S

A, HeLa cells stably expressing hERG-G601S and F-805C were transfected with non-silencing siRNA or with siRNA pools against the indicated protein. Knockdown of the proteins was confirmed by immunoblot. After growth at 27°C for 1 day, CG and FG hERG were detected by Western blotting, and quantified relative to the amount of CG and FG hERG in control conditions (G601S: Bag1, n=5; TRC8, n=7; gp78, n=1; HRD1, n=2; F805C: Bag1, n=6; TRC8, n=7; gp78, n=1; HRD1, n=1).

A

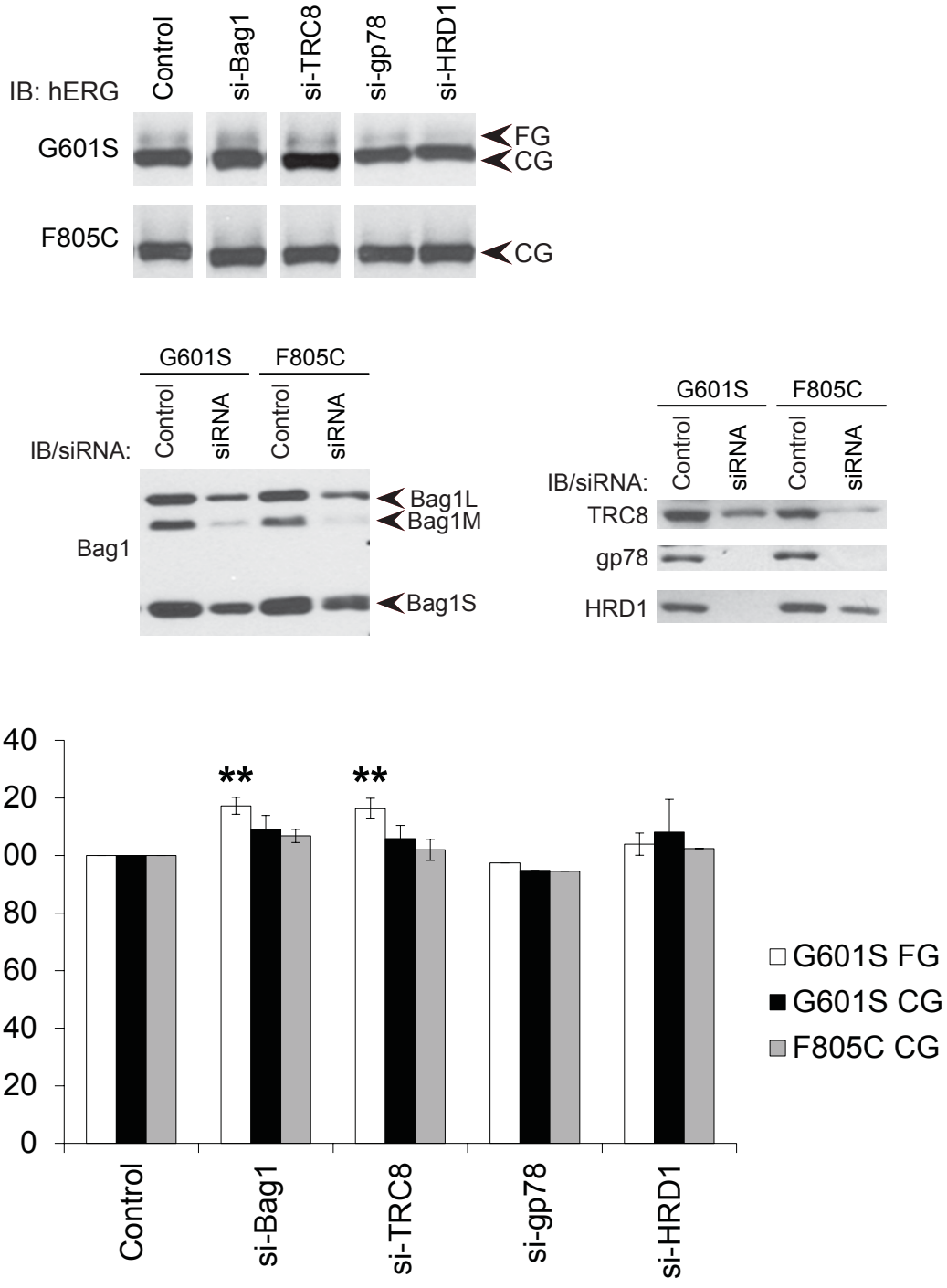
IB: hERG
Control
si-Bag1
si-TRC8
si-gp78
si-HRD1
G601S
F805C
FG
CG
CG
G601S
F805C
IB/siRNA:
Control
siRNA
Control
siRNA
Bag1
Bag1L
Bag1M
Bag1S
G601S
F805C
IB/siRNA:
Control
siRNA
Control
siRNA
TRC8
gp78
HRD1
hERG (% Control)
140
120
100
80
60
40
20
0
**
**
Control
si-Bag1
si-TRC8
si-gp78
si-HRD1
G601S FG
G601S CG
F805C CG

Figure 2.5: A drug-induced stable hERG structure is not degraded by TRC8

A, HEK293 cells were transiently transfected with hERG WT or G601S, and either TRC8 or vector control, grown at 37°C and treated with 5 μM E-4031 or DMSO vehicle control for 24 hours. CG and FG hERG were detected by immunoblot and quantified relative to the amount of CG hERG in control vehicle-treated cells (n=7). B, HeLa cells stably expressing hERG-G601S were treated with E4031 as in B. Total light membrane fractions were isolated and treated with the indicated amounts of trypsin for 10 min at 37°C. CG and FG hERG were detected by immunoblot and quantified relative to the amount without trypsin treatment ($n \geq 4$). Error bars represent standard errors, * $p<0.05$, **$p<0.01$ relative to controls.

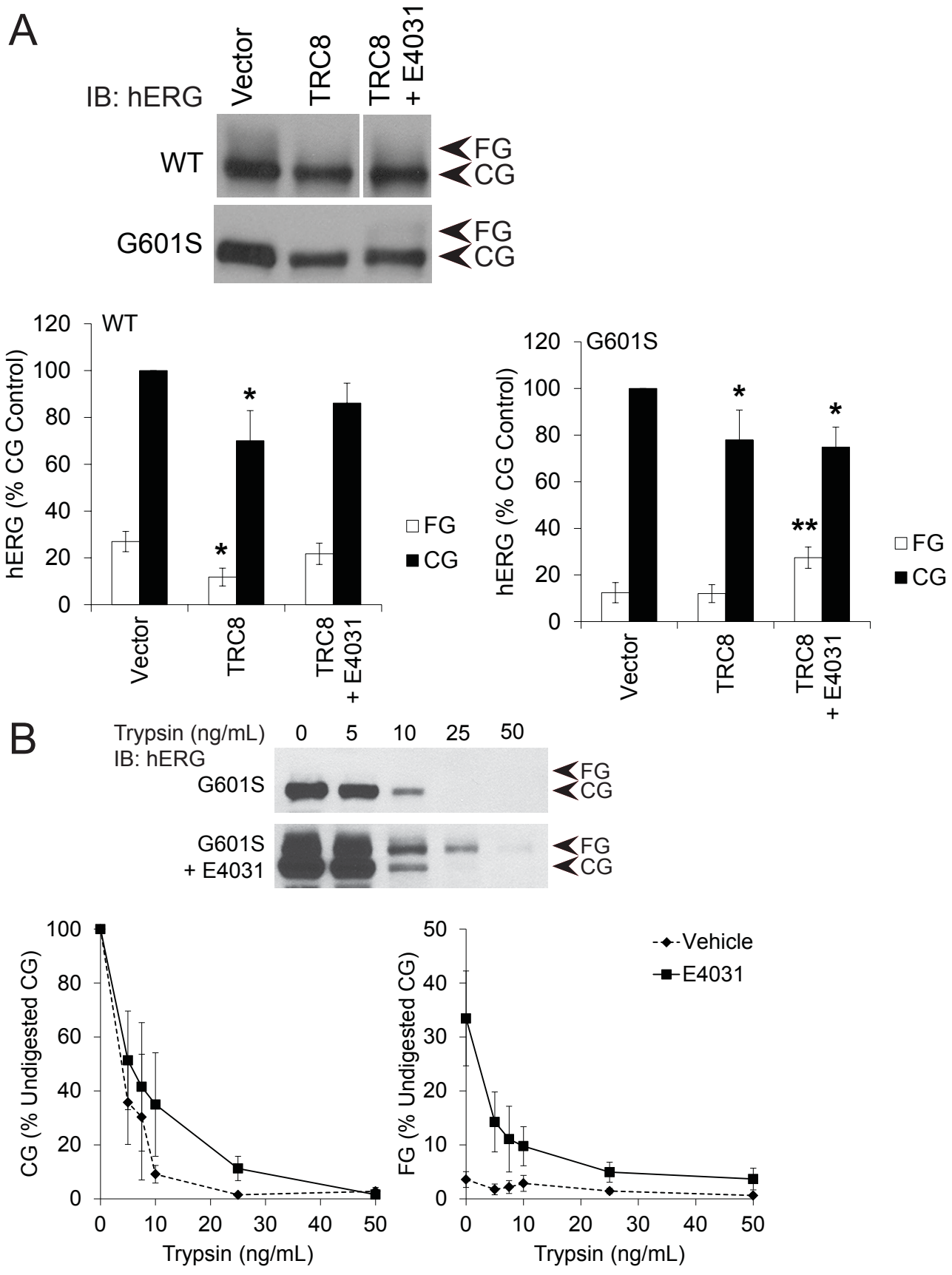
A
IB: hERG
Vector
TRC8
TRC8 + E4031
WT
G601S
FG
CG
WT
G601S
hERG (% CG Control)
120
100
80
60
40
20
0
*
**
FG
CG
Vector
TRC8
TRC8 + E4031
B
Trypsin (ng/mL)
0
5
10
25
50
IB: hERG
G601S
G601S + E4031
CG (% Undigested CG)
FG (% Undigested CG)
Trypsin (ng/mL)
Vehicle
E4031

Derlin-1 promotes hERG degradation

Since ERAD complexes consist of E3 ligases in association with other complimentary proteins, once TRC8 was identified as the ligase for hERG ERAD, we went on to study other cofactors that might work with TRC8 to degrade a misfolded form. Again, we used siRNA screening to perform knockdown of the Derlin family proteins in HeLa cells stably expressing WT-hERG. We found that knocking down Derlin-1 significantly increased the expression of both CG and FG forms of hERG (Figure 2.6A). Derlin3 knockdown did not significantly change the expression of either CG or FG forms of hERG.

Maturation of hERG is lost when Hsp70 is inhibited

We previously observed that loss of Hsp70 by siRNA knockdown resulted in less hERG CG and FG forms (Christine Hantouche, unpublished). Furthermore, when Bag1 overexpression induced a misfolded form of hERG there was less Hsp70 found in complex with immunoprecipitated hERG (Christine Hantouche, unpublished). To determine if Hsp70 specific inhibitors had a similar effect on hERG, we treated HeLa cells stably expressing WT-hERG with DMSO or with 1 μM, 5 μM, or 10 μM of YK198. The CG form of hERG increased with the YK198 treatment concentration and the matured FG form decreased more than 40% with treatment (Figure 2.7A). A slight increase in hERG molecular weight was also observed with all three YK198 treatments.

Figure 2.6: Derlin-1 degrades hERG at the ER

HeLa cells stably expressing WT-hERG were transfected with siRNA against Derlin-1, Derlin-3, or non-silencing control. Knockdown of the proteins was confirmed by Western blot after a 48 hour transfection. CG and FG hERG were detected by immunoblot, and quantified relative to the amount of each in control cells (Derlin-1, n=3; Derlin-3, n=1).

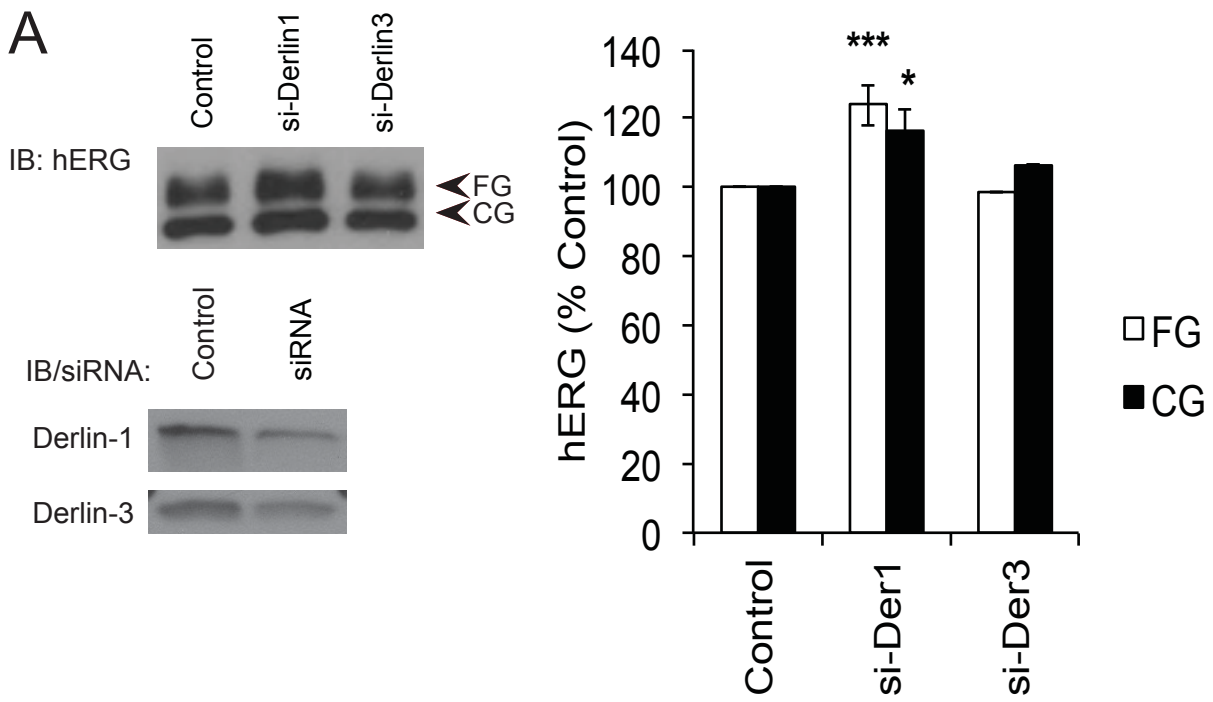
A
Control
si-Derlin1
si-Derlin3
IB: hERG
FG
CG
Control
siRNA
IB/siRNA:
Derlin-1
Derlin-3
hERG (% Control)
140
120
100
80
60
40
20
0
***
*
FG
CG
Control
si-Der1
si-Der3

Figure 2.7: Inhibition of Hsp70 inhibits hERG maturation

HeLa cells stably expressing WT-hERG were treated with 1, 5, or 10 μM of YK198 or an equal volume of DMSO for control. Maturation of hERG was measured by immunoblot after a 24 hour incubation with or without the drug. CG and FG hERG were detected by immunoblot, and quantified relative to the amount of each in control cells (n=3).

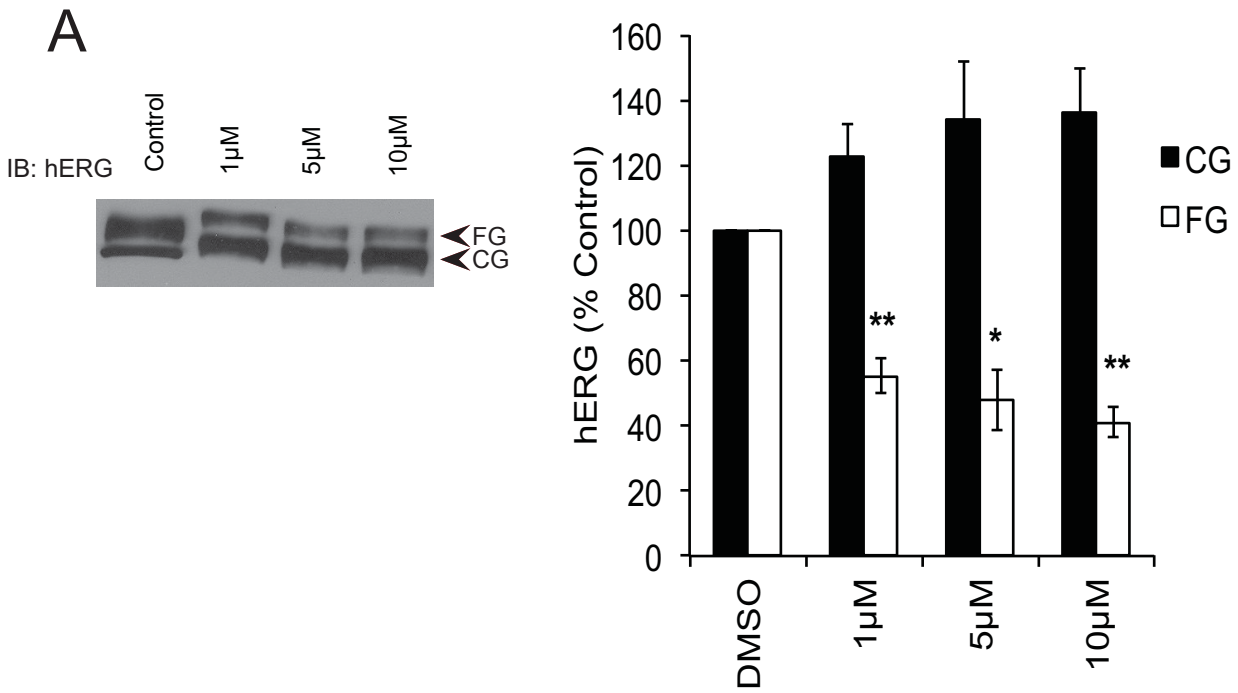
A
IB: hERG
Control
1μM
5μM
10μM
FG
CG
160
140
120
100
80
60
40
20
0
hERG (% Control)
CG
FG
**
*
**
DMSO
1μM
5μM
10μM

Chapter 3

Discussion

We present here a model for hERG degradation that includes a newly identified ERAD complex which preferentially degrades a more heavily misfolded hERG substrate. By determining that the E2 conjugating enzyme Ube2g2 was responsible for the ubiquitination of hERG, its partner ER-bound E3 ligase TRC8 was also identified to play a central role in hERG degradation. Based off of our previous findings where Bag1 induced a less stable, misfolded structure of hERG, we hypothesized that the newly identified TRC8 ligase would preferentially degrade the misfolded hERG substrate. Indeed, TRC8 knockdown increases the FG form of G601S hERG, and a structurally stabilized hERG is not degraded by TRC8 over-expression. We also found that other more studied ER-bound E3 ligases, gp78 and HRD1, do not seem to play a role in hERG degradation, but Derlin-1, a partner with previously identified TRC8 ERAD complexes, does.

Of the ER bound E3 ligases, the presence of TRC8 in degradation complexes has been identified for at least five other substrates: heme oxygenase-1 (HO-1), MHC-I, HMG-CoA reductase, HCV core protein, and XBP1u [61, 74, 75, 77, 79, 81, 82]. TRC8 engages in a regulated role for the ERAD of these substrates, but it also seems to function as a quality control E3 ligase for misfolded proteins such as hERG. Additionally, if these aforementioned TRC8 substrates are presented under a stressed state, it seems plausible

that TRC8 may degrade substrates, such as misfolded hERG, that might induce ER stress if not removed. TRC8 is the first ER-bound quality control E3 ligase identified in potassium channel degradation. It is particularly interesting since the hERG structure is more complex than other TRC8 substrates, which are smaller and single-membrane spanning. In comparison, hERG forms a tetramer, where each oligomer contains six transmembrane segments and large cytosolic domains [10]. It is possible that TRC8 is also involved in the ubiquitination and degradation of other hERG related ion channels, though this has not yet been explored.

Of the previously identified TRC8 substrates, XBP1u, MHC-I molecules and HCV core protein all involve TRC8 interaction with signal peptide peptidase (SPP). While SPP and TRC8 often work together to send substrates for ERAD, in these instances SPP cleaves single transmembrane proteins [81, 82]. We postulate that the multi-transmembrane spanning hERG oligomer and its N-linked glycosylation would likely interfere with SPP interaction, and further, the absence of a large luminal domain reduces the likelihood of SPP cleaving hERG [64]. Although we have yet to experimentally show involvement of SPP in hERG ERAD, we think that it is more likely that TRC8 works independently of SPP by recognizing misfolded substrate through its transmembrane domain, as indicated by our immunoprecipitations. The TRC8-mediated ubiquitination and degradation of HO-1 is facilitated through the transmembrane region as well and its possible that HO-1 and hERG undergo similar mechanisms for interaction and degradation [63]. The degradation of other TRC8 substrates may follow a similar mechanism to what we see with hERG quality control degradation. As discussed previously, upon SPP cleavage the remaining XBP1u fragment is degraded by TRC8

[82], the immature HCV core protein is also quickly degraded by TRC8 if SPP is inhibited [81], and the transmembrane degradation of HO-1 is initiated by SPP cleavage [63]. These TRC8 substrates may be structurally abnormal and since the cleavage and rapid subsequent degradation by TRC8 imitates protein quality control mechanisms, these other substrates may also represent quality control degradation through TRC8 much the way that hERG is. Although TRC8, RING mutant and ΔRING immunoprecipitated with hERG, indicating a transmembrane interaction, there is still a small section of cytosolic TRC8 present in the ΔRING protein, so there is still the potential for a cytosolic interaction with hERG (Figure 2.1A).

Here we show that increasing the expression of TRC8 also increases hERG ubiquitination and its ERAD, consequently lowering FG hERG and its expression as a cell-surface ion channel. The truncated form of TRC8 had no effect, and while the RING-mutant still lowered the trafficking of hERG as seen by decreased FG form, it does not increase hERG ubiquitination. In the catalytically inactive form of TRC8, the zinc finger RING domain contains C547A and C550A mutations, which inhibit its E3-ligase activity by disrupting two Zn^{2+} ion coordinating sites that normally form a binding site for an E2 ubiquitin-conjugating enzyme such as Ube2g2 [84, 90, 91] (Figure 3.1).

Although this RING-mutant ablates ubiquitination activity of TRC8, it might be possible that there is a slight misfolding of the Ube2g2-binding region that exposes hydrophobic residues, thereby preventing ubiquitination, but possibly producing an artifact of retaining substrate at the ER, such as seen with hERG. We saw the same effects in our pulse chase assay as we did with steady state experiments by Western

Figure 3.1: The structure of Ube2g2 bound to the gp78 RING domain

Similar to TRC8, the RING domain of gp78 is the binding site for the partner E2 conjugating enzyme, Ube2g2. Additionally, gp78 contains a G2BR sequence that is not conserved in TRC8. Two mutations in the zinc-binding domain of the RING (blue) would disrupt interaction with Ube2g2 (silver), and prevent transfer of ubiquitin. Image obtained from [90].

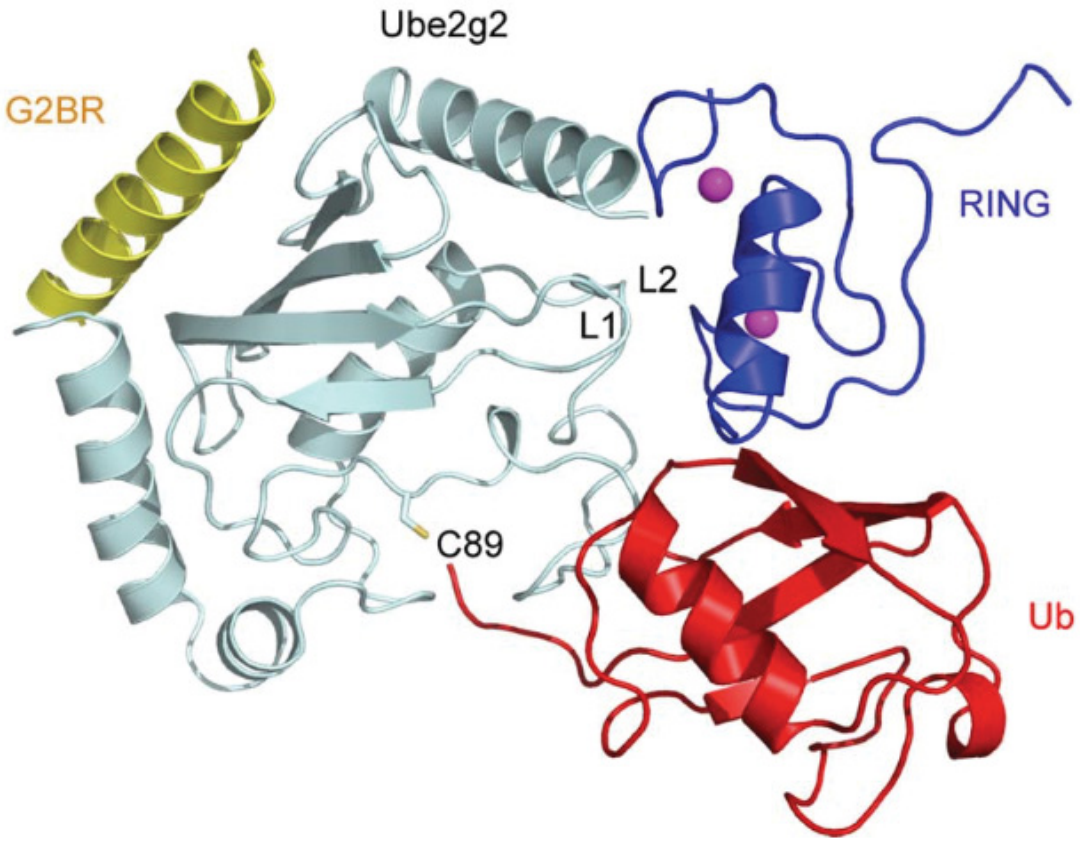

blots, where the ΔRING had no effect, while TRC8 degraded hERG and lowered hERG trafficking. Similarly with our steady state findings, the RING mutant hindered mature hERG formation, perhaps due to hERG being retained and not progressing through to the Golgi, or perhaps hERG is able to exit the ER but goes through lysosomal degradation instead of cell surface trafficking, although we have not confirmed this. Because TRC8 is found only at the ER, the former possibility is more likely.

LQT2 is autosomal dominantly inherited, with mutant oligomers causing dysfunction of the hERG channel. There are hundreds of LQT2 mutations, many of which cause misfolding and inhibit trafficking. Since we identified a condition (Bag1 expression) that induces a misfolded hERG structure which TRC8 degrades, we wanted to determine if TRC8 had a role in regulating the clinically relevant forms of misfolded hERG. Since Bag1 and TRC8 knockdown increased the FG form of G601S hERG and since pharmaceutical restoration of the hERG structure allowed hERG evasion of TRC8 mediated degradation, we propose that TRC8 can act as a quality control E3 ligase for misfolded proteins. This is a new discovery, as it has not been clear that previously known TRC8 substrates are misfolded. Drug-induced stability and restoration of hERG trafficking is promising since it enables hERG to evade degradative mechanisms, though blocking the ion channel must still be corrected for. Interestingly, this effect supports the idea that new ion channel correctors could be developed to promote hERG trafficking and structure stabilization.

Regulation of hERG depends on Hsp70 and Hsp90, where disruption of this interaction can lead to defective hERG biosynthesis. The Hsp70 inhibitor YK198 binding

site is predicted to overlap with the binding sites of NEFs, similar to that of YK5 [92]. As expected with Hsp70 inhibition here, hERG trafficking was inhibited and a more prominent immature form was present. It would be relevant to test if this pharmaceutical inhibition of Hsp70 causes an unstable, misfolded form of hERG at the ER much like what we previously reported with Bag1 overexpression. It is interesting to note that hERG increases proliferation and is up regulated in many cancer types [93], and the use of Hsp70 and Hsp90 activity inhibitors are being developed as potential cancer therapeutics and have been demonstrated to have anti-cancer effects [94-97]. Perhaps these chaperone inhibitors are effective at least in part because of the down regulation of cancer-induced hERG over-expression. Previous work shows that the hERG current is important for neoplastic tumor growth [98] and cell proliferation [93], and is involved in gastric [99] ovarian [100], and endometrial [101] cancers.

To go a step further, perhaps inhibiting Hsp70, much like the Bag1-promoted substrate release, allows the substrate hERG to undergo TRC8-mediated ERAD. Previous works shows that TRC8 expression corresponds with suppressing hereditary renal cancer, and due to its degradation of HO-1, which is also over-expressed in cancer, TRC8 has anti-tumorigenic effects [63, 84]. TRC8 may provide a new means to suppress the progression of those cancers which over-express oncogenic substrates that are degraded through TRC8 ERAD. Since some cancers have suggested a correlation with hERG expression and the progression of cancer, this novel pathway of hERG degradation could provide an alternate means of manipulating cancer progression in cells that highly express hERG.

Furthermore, the cell environment may have implications in hERG folding, not only with stress induced protein folding mechanisms or the K^+ ion concentration [102], but possibly with sterol-induced TRC8 degradation as well. In addition to TRC8 acting as a quality control E3 ligase, it may be able to degrade hERG in response to the cell cholesterol levels. It has been reported that disrupting intracellular cholesterol lowers hERG trafficking to the cell surface and results in an accumulation of CG hERG at the ER [103]. Regulation of cholesterol is important for protein folding, where enhanced cholesterol levels can cause ER stress. In late stage pregnancy for example, progesterone levels are high and induce an accumulation of intracellular cholesterol, which results in inhibited hERG trafficking [103]. TRC8 lowers cholesterol synthesis by degrading HMG-CoAR and SREBP; it is possible that in addition to TRC8 degrading hERG, it may also regulate hERG trafficking by adjusting cholesterol levels. As such, TRC8 may have an influence on the production of arrhythmias by its regulation of physiologically functional hERG through the means of maintaining intracellular cholesterol homeostasis, preventing induction of ER stress pathways, and degrading a misfolded, nonfunctional form of hERG. Of course, the TRC8 E3 ligase role is further complicated by its report of self-ubiquitination [75], therefore providing potential regulation of many physiological events in cholesterol production, cell stress induction, and maturation of substrates such as hERG.

Chapter 4

Materials & Methods

Cell Culture

Cells were grown on polystyrene dishes (Corning) in humid air at 37 °C and 5% CO2. HEK293 cells were maintained in Dulbecco's modified Eagle's medium (DMEM), high glucose and glutamine (Gibco), supplemented with 10% fetal bovine serum (FBS) (Wisent), 100 units/ml Penicillin and 100 μg/ml Streptomycin (Gibco). HeLa cells maintained the stable expression of hERG due to 5ug/mL of puromycin (Gibco). For transfection experiments with HEK293 cells, 60mm or 100mm plates were coated with poly-L-lysine (Sigma) (37 °C for 1h or overnight at 0.1mg/mL in water, followed by one PBS wash).

Plasmids

hERG-pcDNA3.1 with extracellular HA tag positioned on the S1-S2 loop, after residue 443, was a gift from Eckhard Ficker [66]. Point mutations provided the F805C and G601S-hERG-pcDNA3 constructs used for steady state E-4031 experiments. All three TRC8 vectors in pcDNA-HA2 were obtained from Lee-Young Chau. Full length WT-TRC8, catalytically inactive RING mutant with C547A and C550A point mutations, and TRC8 C-terminus truncation (ΔS491) mutant are herein called TRC8, RING-mutant and ΔRING, respectively [63].

DNA transfection

Plasmids were transfected into HEK293 when grown to ~40% confluence on poly-L-lysine coated plates using Lipofectamine 2000 (Invitrogen) with vector-specific parameters optimized through protein expression measured by Western blot. Transfection mixtures were prepared in Opti-MEM (Invitrogen) according to the manufacturers protocol. Transfection of $3x10^6$ HEK293 cells was completed using 6 μg HA-hERG and either 12 μg of WT-TRC8, 4 μg of RING-mutant, or 1 μg of ΔRING, supplemented with pcDNA-HA2 empty vector to bring total DNA to 18μg per 100mm plate. For 60mm plates use in pulse chase experiments, 2 μg of HA-hERG was transfected, with TRC8 constructs adjusted accordingly. For 35mm plates 1 μg of HA-hERG was used, respectively, with TRC8 constructs adjusted accordingly. Briefly, for every μg of plasmid DNA, 1 μL of Lipofectamine 2000 was first mixed into Opti-MEM media. After 10 min, DNA was added to the tubes and gently mixed. Following a 30 min incubation, transfection mixtures were added to cells. After a 6 hour incubation the transfection media was aspirated and warm HEK293 media (DMEM-FBS) was added and the cells were returned to normal growth conditions for 2 days.

siRNA transfection

HeLa hERG stably expressing cells were transfected when grown to ~30% confluence using Oligofectamine (Invitrogen) and gene-specific ON-TARGETplus SMARTpool siRNA (Dharmacon-GE Health). A total amount of 1.25umol of siRNA was used to transfect 35-mm plates, where knock down of two genes required 0.625μM of each target siRNA. Briefly, 2.5μL of Oligofectamine was first mixed into Opti-MEM

(Invitrogen) media. After 10 min, siRNA was first mixed into 100μL Opti-MEM and then gently mixed with the Oligofectamine mixture. Following a 30 min incubation, transfection mixtures were added to cells, which were prewashed two times with Opti-MEM. After a 6 hour incubation the transfection media was aspirated and warm HeLa media (DMEM-FBS-Puro-PS) was added and the cells were returned to normal growth conditions for 2 days. For multi-day transfections, a plate of ~70% confluence was transfected, split after the 6 hr incubation and plated into different confluencies as to permit multi-day lysing and confirmation of the optimal day for siRNA knockdown.

siRNAs

All siRNA duplexes were from Dharmacon/Thermo Fisher Scientific in smart pools with the following target sequences:

ON-Target plus non-targeting siRNA pool (D-001810-10-05)
5'-UGGUUUACAUGUCGACUAA
5'-UGGUUUACAUGUUGUGUGA
5'-UGGUUUACAUGUUUUCUGA
5'-UGGUUUACAUGUUUUCCUA

TRC8 (RNF139) (L-006942-00-0005)
5'-UGACAGGCGUCUUGGCUUU
5'-GGGAGCCGCUUACAAGAAA
5'-AGAGAGACUUUACUGUUUA
5'-GGGAAAAGCUUGACGAUUA

gp78 (AMFR) (L-006522-00-0005)
5'-GCAAGGAUCGAUUUGAAUA
5'-GGACGUAUGUCUAUUACAC
5'-GAAUUCGUCGGCACAAGAA
5'-GUAAAUACCGCUUGCUGUG

HRD1 (SYVN1) (L-007090-00-0005)
5'-GGAAAGGCCUCCAGCUCCU
5'-CAACAUGAACACCCUGUAU

5’-GAGAAGAGAUGGUGACUGG
5’-UCAUCAAGGUUCUGCUGUA

RMA1 (RNF5) (L-006558-00-0005)
5’-GGCCAUGUCUUCAUCAGUG
5’-GCAAGAGUGUCCAGUAUGU
5’-UCAAUGCCCAUGAGCCUUU
5’GCGCGACCUUCGAAUGUAA

CHIP (STUB1) (L-007201-00-0005)
5’-CGCUGGUGGCCGUGUAUUA
5’-GUGGAGGACUACUGAGGUU
5’-GAAGGAGGUUAUUGACGCA
5’-UGGAAGAGUGCCAGCGAAAA

UBE2G2 (L-009095-00-0005)
5’-GAUGGGAGAGUCUGCAUUU
5’-GAGCUAACGUGGAUGCGUC
5’-GCGAUGACCGGGAGCAGUU
5’-CCACUUGAUUACCCGUUAA

Derlin1 (L-010733-02-0005)
5’- GGGCCAGGGCUUUCGACUU
5’- CAAUUAUGUUGCACGUACA
5’-GAGAGACCCUCAUACGCUA
5’-CAACAAUCAUAUUCACGUA

Derlin-2 (L- 010576-01-0005)
5’ –CUAUAUCGUUACUGUCGAA
5’- GUCUAUGUGUGGAGCCGAA
5’- CUGCAGAUCCCACCGGUCA
5’ – AGGACAAAAUAAAACGGAA

Derlin-3 (L-032237-01-0005)
5’-GGGUCAACUUCUUCGGCCU
5’- GGGAUUGCGGUGGGCCAUA
5’-UCUGGAGGCUCGUCACCAA
5’-GAACAAACACCUCAGCAAU

Co-Immunoprecipitation

HEK293 cells were plated in 10-cm poly-L-lysine (Sigma) coated dishes and transfected with hERG and TRC8 plasmids as previously described. After 48 hours, cells

were lysed as described above in 0.1% Triton 100-X lysis buffer. The normalized supernatant was incubated with 5 μg of mouse monoclonal anti-hERG antibody (Alomone) for 1.5 hours at 4 °C. After incubation, 50μL of 50% Protein G-Agarose Fast Flow slurry (EMD Millipore) in 0.1% lysis buffer was added to the sample and rocked for another 1.5 hrs at 4 °C. The beads were centrifuged briefly and the flow through was collected and snap frozen. The beads were washed with 0.1% lysis buffer for a minimum of five times. After an addition of 60μL Laemmli loading buffer, the beads were incubated at 65°C for 30 minutes. The supernatant was collected and subjected to SDS-PAGE and Western blot analysis. For blotting detection, mouse monoclonal anti-TRC8 (Abcam) 1:1000, and mouse monoclonal anti-HA (Sigma-Aldrich) 1:4000 were used.

Ubiquitination

To detect polyubiquitination hERG, the co-immunoprecipitation protocol was followed as above, with the exception of the lysis buffer. Here, the 0.1% lysis and wash buffers contained 5mM N-Ethylmaleimide (NEM) (Sigma-Aldrich) to inhibit deubiquitinating enzyme in the cell lysate. To blot for ubiquitin, the primary antibody anti-ubiquitin PD41 (Santa Cruz) 1:5000 was used.

Western Blot

Cells were lysed after 48 hr transient transfection of plasmid or siRNA. Cells were washed two times with ice-cold PBS pH 7.4, scraped in 1mL PBS, and added to pre-cooled sample tube. Samples were centrifuged at 1000 x g for 5 min at 4 °C and

supernatant aspirated. The pellet was resuspended in cold lysis buffer (PBS, 1% Triton X-100, and protease inhibitor cocktail [Roche]). After incubating for 10 min on ice, the supernatant was collected by centrifugation at 20,000 x g for 10 minute at 4 °C.

Samples were then taken for protein concentration measurement (BioRad DC™ Protein Assay Kit), and total lysate samples were normalized with lysis buffer. Laemmli loading buffer (0.1 M Tris pH 6.8, 10% glycerol, 10% SDS, 10% 2-mercaptoethanol) was added to all samples and denatured at 65°C for 15 min. Proteins were separated by 7,10, or 15% acrylamide sodium dodecyl sulfate poly acrylamide gel electrophoresis (SDS-PAGE).

After SDS-PAGE, proteins were electro-transferred to nitrocellulose membrane (BioRad) in transfer buffer (500mM Glycine, 50mM Tris-HCl, 0.01% SDS, 10% methanol) at 200mA for 2 hours.

Membranes were blocked with 5% skim milk (for mono-clonal antibodies) or BSA (for poly-clonal antibodies) PBS-T for 1 hour at room temperature. Membranes are incubated with primary antibody in 5% skim milk or BSA PBS-T at 4 °C over night, or for 1 hour at room temperature. Membranes were washed with PBS-T for 10 min three times. Membranes were then incubated for 1h at room temperature with either goat anti-mouse IgG constant fragment conjugated to horseradish peroxidase (Jackson ImmunoResearch) at 1:10,000 dilution or goat anti-rabbit IgG constant fragment conjugated to horseradish peroxidase (Jackson ImmunoResearch) at 1:10, 000 dilution unless otherwise stated. After 1 h incubation, membranes were again washed three times for ten minutes in PBS-T. Detection of signal was carried out by providing substrate with ECL™ blotting detection reagents (GE Healthcare), and using traditional film-based exposure and development methods or by a FluorChem HD2 digital camera (Alpha Innotech).

Antibodies

Mouse monoclonal anti-RNF139 (TRC8) 1:1000, mouse monoclonal anti-STUB1 (CHIP) 1:10, 000, mouse monoclonal anti-AMFR (Gp78) 1:2000, rabbit polyclonal anti-SYVN1 (Hrd1) 1:5000, mouse monoclonal anti-Ube2g2 1:1000 antibodies were obtained from Abcam. Rabbit polyclonal anti-Derlin-1 1:10000, rabbit polyclonal anti-Derlin-2 1:5000, rabbit polyclonal anti-Derlin-3 1:1000, rabbit polyclonal anti-RNF139 1:1000, mouse monoclonal anti-Bag1 1:500, mouse monoclonal anti-Hemagglutinin 1:4000, mouse monoclonal anti-Hsp70 1:20, 000 and mouse monoclonal anti-Tubulin 1:20000 were obtained from Sigma-Aldrich. Mouse monoclonal anti-Ubiquitin (P4D1) 1:100 was obtained from Santa Cruz. Goat anti-rabbit IgG conjugated HRP and Goat anti-mouse IgG conjugated HRP were obtained from Jackson ImmunoReseach Laboratory. For immunoprecipitations, rabbit polyclonal anti-hERG from Alomone Labs was used.

Limited Proteolysis

HeLa WT-hERG and G601S-hERG cell lines were grown in 100mm dishes supplemented DMEM media with or without E-4031 (Sigma) to ~90% confluence. Cells were washed twice in ice-cold PBS- 0.1mM Ca^{2+} 1mM Mg^{2+}. Cells were scraped off into a falcon tube and were centrifuged at 4°C in a JS-5.3 rotor (Beckman Coulter Avanti J-26 XP centrifuge) at 2,000 rpm for 2 min. The pellet was resuspended in sucrose washing solution (0.25M sucrose, 10mM HEPES-KOH pH 6.8 and 1mM EDTA). Following centrifugation at 4°C using a JS-5.3 rotor at 4,000 rpm for 5 min, the pellet was

resuspended in 0.25M sucrose, 10mM HEPES-KOH, 1mM EDTA, 10μg/mL Leupeptin, 10μg/mL Pepstatin, and 1mM DTT. Homogenate was lysed at 20 BAR using a nitrogen homogenization bomb (4635 Cell Disruption Vessel, Parr Instruments). The nuclei was separated by centrifugation in a SX4750 rotor (Beckman Coulter Allegra X-ISR) at 4,000 rpm for 5 min at 4°C. The mitochondria was removed from that supernatant by centrifugation at 9,000 rpm at 4°C in a JA-20 rotor (Beckman Coulter Avanti J-E). The supernatant was centrifuged for 1 h at 23,000 rpm at 4°C in a Ti90 rotor (Beckman Coulter Optima L-80 XP Ultracentrifuge). The microsomal pellet was resuspended in 0.25 M sucrose, 10 mM HEPES-KOH pH 7.6, and 1 mM EDTA, and flash frozen in 200μL aliquots. For proteolytic digest, microsomal sample was digested for 10 min in 37°C water bath with varying concentrations of trypsin (Worthington) and the reaction was inhibited with 10 mg/mL trypsin inhibitor (Sigma Aldrich), 2 mM PMSF, 10 μg/mL Leupeptin, 10 μg/mL Pepstatin, and 2 mM $MgCl_2$. The samples were run on SDS-PAGE and blotted for hERG using monoclonal anti-HA (Sigma Aldrich).

Pulse Chase

HEK293 cells were transfected with WT-hERG and either WT-TRC8 or RING mutant, or ΔRING. Forty-eight hours post transfected, sub-confluent cell monolayers in 100mm dishes were incubated for one hour in cysteine-free medium (Invitrogen). Cells were labeled for 30 min with 100uCi of [^{35}S]-methionine/cysteine (Perkin-Elmer) and were chased with DMEM media (supplemented with $CaCl_2$ 0.1mM and $MgCl_2$ 1mM) for up to 6 hours. Cells were harvested every two hours in 1% PBS-Triton buffer supplemented with protease inhibitor cocktail. Lysates were immunoprecipitated with

hERG as described above and were eluted in 40μL of Laemmli loading buffer and separated by a 7% SDS-PAGE and analyzed by phosphorimager quantitation. Core glycosylated (CG) values were measured as a percent of control at T=0, and fully glycosylated (FG) values were measured as a percent of the core glycosylated at T=0.

Densitometry

Densitometric analysis of blots was carried out using ImageJ (National Institutes of Health, version 2.00 (8-bit), Bethesda, MD) to measure the relative density of protein amount with respect to control samples. Statistical significance of the results was analyzed by independent samples t-test. A P-value of <0.05 was used to determine statistical significance.

Patch clamp

For plasmid transfections, GFP was co-transfected to identify expressing cells. The cells were plated in the perfusion chamber of an inverted microscope (Zeiss Axiovert S100TV) and perfused with a Tyrodes solution containing 135 mM NaCl, 5 mM KCl, 1 mM $CaCl_2$, 1 mM $MgCl_2$, 10 mM glucose and 5 mM HEPES-NaOH pH 7.4 (300 mOsm). Borosilicate glass pipettes (Warner Instruments) were made using a microprocessor-controlled, multi-stage puller (P97, Sutter Instruments). Tips with resistances between 1.5-3 MΩ were backfilled using an internal solution containing 135 mM KCl, 5 mM EGTA, 1 mM $MgCl_2$ and 5 mM HEPES-KOH pH 7.2 (300 mOsm). All voltage-clamp experiments were performed under the whole-cell configuration at 22°C. Currents were

recorded using an Axon Instruments headstage (CV 203BU), attached to an Axopatch 200B amplifier (Axon Instruments), and displayed on a computer using pClamp 10.2/Digidata 1440A software (Axon Instruments). Data was sampled at 20 kHz (every 50 μs) and filtered at 2 kHz. Prior to the formation of a multi-GΩ seal, currents were corrected for pipette (fast) capacitance. To determine whole-cell capacitance, capacitive currents were elicited by a 30 ms, 10 mV depolarizing pulse from a holding potential of -80 mV at 2 Hz after a whole-cell environment was formed. A minimum requirement for data collection was that access resistance was below 10 MΩ. All currents were corrected for whole-cell capacitance and series resistance was compensated to 80% using the Axopatch 200B amplifier. To obtain tail currents, depolarizing steps (7 s) were imposed from a −80 mV holding potential in increments of 10 mV up to +70 mV, followed by a step back to −50 mV (2 s), which provoked the tail currents. Subsequently, the membrane was clamped back to −80 mV holding potential for 1 s before the next depolarizing step. All tail current values were normalized to cellular capacitance (picofarads) and presented in current/voltage (I/V) relationships. All currents were analyzed in Clampfit 10.2 (Axon Instruments).

References

1. Government of Canada. *Heart Disease - Heart Health*. 2015 [cited 2016 30 March]; Available from: http://healthycanadians.gc.ca/diseases-conditions-maladies-affections/disease-maladie/heart-disease-eng.php.
2. Sandeep K Goyal, M. *Ventricular Fibrillation*. 2014 [cited 2016 May 3, 2016]; Available from: http://emedicine.medscape.com/article/158712-overview.
3. Koplan, B.A. and W.G. Stevenson, *Ventricular Tachycardia and Sudden Cardiac Death.* Mayo Clin Proc, 2009. **84**(3): p. 289-97.
4. Jatin Dave, M. *Torsade de Pointes*. 2015 [cited 2016 May 3]; Available from: http://emedicine.medscape.com/article/1950863-overview.
5. Keating, M.T. and M.C. Sanguinetti, *Molecular and cellular mechanisms of cardiac arrhythmias.* Cell, 2001. **104**(4): p. 569-80.
6. Modell, S.M. and M.H. Lehmann, *The long QT syndrome family of cardiac ion channelopathies: A HuGE review*.* Genetics in Medicine, 2006. **8**(3): p. 143-155.
7. Fermini, B. and A.A. Fossa, *The impact of drug-induced QT interval prolongation on drug discovery and development.* Nat Rev Drug Discov, 2003. **2**(6): p. 439-447.
8. Sanguinetti, M.C. and M. Tristani-Firouzi, *hERG potassium channels and cardiac arrhythmia.* Nature, 2006. **440**(7083): p. 463-9.
9. Jones, D.K., et al., *hERG 1b is critical for human cardiac repolarization.* Proc Natl Acad Sci U S A, 2014. **111**(50): p. 18073-7.
10. Vandenberg, J.I., et al., *hERG K(+) channels: structure, function, and clinical significance.* Physiol Rev, 2012. **92**(3): p. 1393-478.
11. Foo, B., et al., *hERG quality control and the long QT syndrome.* J Physiol, 2016. **594**(9): p. 2469-81.
12. Witchel, H.J., *Drug-induced hERG block and long QT syndrome.* Cardiovasc Ther, 2011. **29**(4): p. 251-9.
13. Zunkler, B.J., *Human ether-a-go-go-related (HERG) gene and ATP-sensitive potassium channels as targets for adverse drug effects.* Pharmacol Ther, 2006. **112**(1): p. 12-37.
14. Schwartz, P.J., et al., *Prevalence of the congenital long-QT syndrome.* Circulation, 2009. **120**(18): p. 1761-7.
15. Anderson, C.L., et al., *Large-scale mutational analysis of Kv11.1 reveals molecular insights into type 2 long QT syndrome.* Nat Commun, 2014. **5**: p. 5535.
16. Apaja, P.M., et al., *Ubiquitination-dependent quality control of hERG K+ channel with acquired and inherited conformational defect at the plasma membrane.* Mol Biol Cell, 2013. **24**(24): p. 3787-804.
17. Young, J.C., *The role of the cytosolic HSP70 chaperone system in diseases caused by misfolding and aberrant trafficking of ion channels.* Dis Model Mech, 2014. **7**(3): p. 319-29.

18. Braakman, I. and N.J. Bulleid, *Protein folding and modification in the mammalian endoplasmic reticulum.* Annual review of biochemistry, 2011. **80**: p. 71-99.
19. Lodish H, B.A., Zipursky SL, et al., *Molecular Cell Biology. 4th edition.* 2000, New York: W. H. Freeman.
20. Hartl, F.U., A. Bracher, and M. Hayer-Hartl, *Molecular chaperones in protein folding and proteostasis.* Nature, 2011. **475**(7356): p. 324-32.
21. Bukau, B. and A.L. Horwich, *The Hsp70 and Hsp60 chaperone machines.* Cell, 1998. **92**(3): p. 351-66.
22. Bertelsen, E.B., et al., *Solution conformation of wild-type E. coli Hsp70 (DnaK) chaperone complexed with ADP and substrate.* Proc Natl Acad Sci U S A, 2009. **106**(21): p. 8471-6.
23. Kityk, R., et al., *Structure and dynamics of the ATP-bound open conformation of Hsp70 chaperones.* Mol Cell, 2012. **48**(6): p. 863-74.
24. Qi, R., et al., *Allosteric opening of the polypeptide-binding site when an Hsp70 binds ATP.* Nat Struct Mol Biol, 2013. **20**(7): p. 900-7.
25. Woo, H.-J., et al., *ATP-induced conformational changes in Hsp70: molecular dynamics and experimental validation of an in silico predicted conformation.* Biochemistry, 2009. **48**(48): p. 11470-11477.
26. Zhuravleva, A., E.M. Clerico, and L.M. Gierasch, *An interdomain energetic tug-of-war creates the allosterically active state in Hsp70 molecular chaperones.* Cell, 2012. **151**(6): p. 1296-307.
27. Bracher, A. and J. Verghese, *The nucleotide exchange factors of Hsp70 molecular chaperones.* Front Mol Biosci, 2015. **2**: p. 10.
28. Scheufler, C., et al., *Structure of TPR domain-peptide complexes: critical elements in the assembly of the Hsp70-Hsp90 multichaperone machine.* Cell, 2000. **101**(2): p. 199-210.
29. Li, J. and J. Buchner, *Structure, function and regulation of the hsp90 machinery.* Biomed J, 2013. **36**(3): p. 106-17.
30. Ballinger, C.A., et al., *Identification of CHIP, a novel tetratricopeptide repeat-containing protein that interacts with heat shock proteins and negatively regulates chaperone functions.* Mol Cell Biol, 1999. **19**(6): p. 4535-45.
31. Meacham, G.C., et al., *The Hsc70 co-chaperone CHIP targets immature CFTR for proteasomal degradation.* Nat Cell Biol, 2001. **3**(1): p. 100-5.
32. Connell, P., et al., *The co-chaperone CHIP regulates protein triage decisions mediated by heat-shock proteins.* Nat Cell Biol, 2001. **3**(1): p. 93-6.
33. Braakman, I. and D.N. Hebert, *Protein folding in the endoplasmic reticulum.* Cold Spring Harb Perspect Biol, 2013. **5**(5): p. a013201.
34. Ali, M.M., et al., *Crystal structure of an Hsp90-nucleotide-p23/Sba1 closed chaperone complex.* Nature, 2006. **440**(7087): p. 1013-7.
35. Shiau, A.K., et al., *Structural Analysis of E. coli hsp90 reveals dramatic nucleotide-dependent conformational rearrangements.* Cell, 2006. **127**(2): p. 329-40.
36. Mickler, M., et al., *The large conformational changes of Hsp90 are only weakly coupled to ATP hydrolysis.* Nat Struct Mol Biol, 2009. **16**(3): p. 281-6.

37. Li, J., J. Soroka, and J. Buchner, *The Hsp90 chaperone machinery: conformational dynamics and regulation by co-chaperones.* Biochim Biophys Acta, 2012. **1823**(3): p. 624-35.
38. Wang, M. and R.J. Kaufman, *The impact of the endoplasmic reticulum protein-folding environment on cancer development.* Nat Rev Cancer, 2014. **14**(9): p. 581-597.
39. Schröder, M. and R.J. Kaufman, *ER stress and the unfolded protein response.* Mutation Research/Fundamental and Molecular Mechanisms of Mutagenesis, 2005. **569**(1–2): p. 29-63.
40. Shen, J., et al., *ER stress regulation of ATF6 localization by dissociation of BiP/GRP78 binding and unmasking of Golgi localization signals.* Dev Cell, 2002. **3**(1): p. 99-111.
41. Hetz, C., *The unfolded protein response: controlling cell fate decisions under ER stress and beyond.* Nat Rev Mol Cell Biol, 2012. **13**(2): p. 89-102.
42. Araki, K. and K. Nagata, *Protein Folding and Quality Control in the ER.* Cold Spring Harbor Perspectives in Biology, 2011. **3**(11): p. a007526.
43. Molinari, M., et al., *Role of EDEM in the release of misfolded glycoproteins from the calnexin cycle.* Science, 2003. **299**(5611): p. 1397-1400.
44. Aebi, M., et al., *N-glycan structures: recognition and processing in the ER.* Trends in Biochemical Sciences, 2010. **35**(2): p. 74-82.
45. Otero, J.H., B. Lizak, and L.M. Hendershot, *Life and death of a BiP substrate.* Semin Cell Dev Biol, 2010. **21**(5): p. 472-8.
46. Berndsen, C.E. and C. Wolberger, *New insights into ubiquitin E3 ligase mechanism.* Nat Struct Mol Biol, 2014. **21**(4): p. 301-7.
47. Haas, A.L. and I.A. Rose, *THE MECHANISM OF UBIQUITIN ACTIVATING ENZYME - A KINETIC AND EQUILIBRIUM-ANALYSIS.* Journal of Biological Chemistry, 1982. **257**(17): p. 329-337.
48. Amm, I., T. Sommer, and D.H. Wolf, *Protein quality control and elimination of protein waste: The role of the ubiquitin–proteasome system.* Biochimica et Biophysica Acta (BBA) - Molecular Cell Research, 2014. **1843**(1): p. 182-196.
49. Araki, K. and K. Nagata, *Protein folding and quality control in the ER.* Cold Spring Harb Perspect Biol, 2011. **3**(11): p. a007526.
50. van den Boomen, D.J. and P.J. Lehner, *Identifying the ERAD ubiquitin E3 ligases for viral and cellular targeting of MHC class I.* Mol Immunol, 2015. **68**(2 Pt A): p. 106-11.
51. Hampton, R.Y. and T. Sommer, *Finding the will and the way of ERAD substrate retrotranslocation.* Curr Opin Cell Biol, 2012. **24**(4): p. 460-6.
52. Wójcik, C., et al., *Valosin-containing Protein (p97) Is a Regulator of Endoplasmic Reticulum Stress and of the Degradation of N-End Rule and Ubiquitin-Fusion Degradation Pathway Substrates in Mammalian Cells.* Molecular Biology of the Cell, 2006. **17**(11): p. 4606-4618.
53. Roy, C.R., S.P. Salcedo, and J.-P.E. Gorvel, *Pathogen–endoplasmic-reticulum interactions: in through the out door.* Nat Rev Immunol, 2006. **6**(2): p. 136-147.
54. Wiertz, E.J., et al., *The human cytomegalovirus US11 gene product dislocates MHC class I heavy chains from the endoplasmic reticulum to the cytosol.* Cell, 1996. **84**(5): p. 769-779.

55. Ye, Y., et al., *A membrane protein complex mediates retro-translocation from the ER lumen into the cytosol.* Nature, 2004. **429**(6994): p. 841-847.
56. Younger, J.M., et al., *Sequential quality-control checkpoints triage misfolded cystic fibrosis transmembrane conductance regulator.* Cell, 2006. **126**(3): p. 571-82.
57. Morito, D., et al., *Gp78 cooperates with RMA1 in endoplasmic reticulum-associated degradation of CFTRDeltaF508.* Mol Biol Cell, 2008. **19**(4): p. 1328-36.
58. Matsumura, Y., L.L. David, and W.R. Skach, *Role of Hsc70 binding cycle in CFTR folding and endoplasmic reticulum-associated degradation.* Mol Biol Cell, 2011. **22**(16): p. 2797-809.
59. Wojcikiewicz, R.J.H., et al., *WHEN WORLDS COLLIDE: IP(3) RECEPTORS AND THE ERAD PATHWAY.* Cell calcium, 2009. **46**(3): p. 147-153.
60. Song, B.-L., N. Sever, and R.A. DeBose-Boyd, *Gp78, a Membrane-Anchored Ubiquitin Ligase, Associates with Insig-1 and Couples Sterol-Regulated Ubiquitination to Degradation of HMG CoA Reductase.* Molecular Cell, 2005. **19**(6): p. 829-840.
61. Jo, Y., et al., *Sterol-induced degradation of HMG CoA reductase depends on interplay of two Insigs and two ubiquitin ligases, gp78 and Trc8.* Proceedings of the National Academy of Sciences, 2011. **108**(51): p. 20503-20508.
62. Kim, H.P., et al., *Heme oxygenase-1 comes back to endoplasmic reticulum.* Biochemical and Biophysical Research Communications, 2011. **404**(1): p. 1-5.
63. Lin, P.H., W.M. Lan, and L.Y. Chau, *TRC8 suppresses tumorigenesis through targeting heme oxygenase-1 for ubiquitination and degradation.* Oncogene, 2013. **32**(18): p. 2325-2334.
64. Boname, J.M., et al., *Cleavage by signal peptide peptidase is required for the degradation of selected tail-anchored proteins.* J Cell Biol, 2014. **205**(6): p. 847-62.
65. Soto, C., *Unfolding the role of protein misfolding in neurodegenerative diseases.* Nat Rev Neurosci, 2003. **4**(1): p. 49-60.
66. Ficker, E., et al., *Role of the cytosolic chaperones Hsp70 and Hsp90 in maturation of the cardiac potassium channel HERG.* Circ Res, 2003. **92**(12): p. e87-100.
67. Walker, V.E., et al., *Hsp40 chaperones promote degradation of the HERG potassium channel.* J Biol Chem, 2010. **285**(5): p. 3319-29.
68. Iwai, C., et al., *Hsp90 prevents interaction between CHIP and HERG proteins to facilitate maturation of wild-type and mutant HERG proteins.* Cardiovasc Res, 2013. **100**(3): p. 520-8.
69. Li, P., et al., *Reciprocal control of hERG stability by Hsp70 and Hsc70 with implication for restoration of LQT2 mutant stability.* Circ Res, 2011. **108**(4): p. 458-68.
70. Roder, K., et al., *RING finger protein RNF207, a novel regulator of cardiac excitation.* J Biol Chem, 2014. **289**(49): p. 33730-40.
71. Po-Chiao Chang, H.-W.T., Ming-Tsai Chiang, Pei-Ling Huang, Song-Kun Shyue, Lee-Young Chau, *TRC8 downregulation contributes to the development of non-*

alcoholic steatohepatitis by exacerbating hepatic endoplasmic reticulum stress. Biochimica et Biophysica Acta, 2015. **1852**: p. 2339-2351.
72. Daemen, S., M. Kutmon, and C.T. Evelo, *A pathway approach to investigate the function and regulation of SREBPs.* Genes & Nutrition, 2013. **8**(3): p. 289-300.
73. Brown, M.S. and J.L. Goldstein, *The SREBP pathway: regulation of cholesterol metabolism by proteolysis of a membrane-bound transcription factor.* Cell, 1997. **89**(3): p. 331-40.
74. Hwang, S., et al., *Contribution of accelerated degradation to feedback regulation of 3-hydroxy-3-methylglutaryl coenzyme a reductase and cholesterol metabolism in liver.* Journal of Biological Chemistry, 2016.
75. Irisawa, M., et al., *The sterol-sensing endoplasmic reticulum (ER) membrane protein TRC8 hampers ER to Golgi transport of sterol regulatory element-binding protein-2 (SREBP-2)/SREBP cleavage-activated protein and reduces SREBP-2 cleavage.* Journal of Biological Chemistry, 2009. **284**(42): p. 28995-29004.
76. Yang, T., et al., *Crucial step in cholesterol homeostasis: sterols promote binding of SCAP to INSIG-1, a membrane protein that facilitates retention of SREBPs in ER.* Cell, 2002. **110**(4): p. 489-500.
77. Lee, J.P., et al., *The TRC8 ubiquitin ligase is sterol regulated and interacts with lipid and protein biosynthetic pathways.* Molecular Cancer Research, 2010. **8**(1): p. 93-106.
78. Law, M.R., N.J. Wald, and A. Rudnicka, *Quantifying effect of statins on low density lipoprotein cholesterol, ischaemic heart disease, and stroke: systematic review and meta-analysis.* Bmj, 2003. **326**(7404): p. 1423.
79. Stagg, H.R., et al., *The TRC8 E3 ligase ubiquitinates MHC class I molecules before dislocation from the ER.* J Cell Biol, 2009. **186**(5): p. 685-92.
80. Lilley, B.N.a.P., H.L. , *A membrane protein required for dislocation of misfolded proteins from the ER.* Nature 2004. **429**: p. 834 - 840.
81. Aizawa, S., et al., *TRC8-dependent degradation of hepatitis C virus immature core protein regulates viral propagation and pathogenesis.* Nat Commun, 2016. **7**: p. 11379.
82. Chen, C.Y., et al., *Signal peptide peptidase functions in ERAD to cleave the unfolded protein response regulator XBP1u.* Embo j, 2014. **33**(21): p. 2492-506.
83. Yanagitani, K., et al., *Translational pausing ensures membrane targeting and cytoplasmic splicing of XBP1u mRNA.* Science, 2011. **331**(6017): p. 586-9.
84. Brauweiler, A., et al., *RING-dependent tumor suppression and G2//M arrest induced by the TRC8 hereditary kidney cancer gene.* Oncogene, 2006. **26**(16): p. 2263-2271.
85. Akhavan, A., et al., *Identification of the cyclic-nucleotide-binding domain as a conserved determinant of ion-channel cell-surface localization.* J Cell Sci, 2005. **118**(Pt 13): p. 2803-12.
86. Anderson, C.L., et al., *Most LQT2 mutations reduce Kv11.1 (hERG) current by a class 2 (trafficking-deficient) mechanism.* Circulation, 2006. **113**(3): p. 365-73.
87. Ficker, E., et al., *The binding site for channel blockers that rescue misprocessed human long QT syndrome type 2 ether-a-gogo-related gene (HERG) mutations.* Journal of Biological Chemistry, 2002. **277**(7): p. 4989-4998.

88. Gong, Q., M.A. Jones, and Z. Zhou, *Mechanisms of pharmacological rescue of trafficking-defective hERG mutant channels in human long QT syndrome.* Journal of Biological Chemistry, 2006. **281**(7): p. 4069-4074.
89. Zhou, Z., Q. Gong, and C.T. January, *Correction of defective protein trafficking of a mutant HERG potassium channel in human long QT syndrome Pharmacological and temperature effects.* Journal of Biological Chemistry, 1999. **274**(44): p. 31123-31126.
90. Li, W., et al., *Mechanistic insights into active site-associated polyubiquitination by the ubiquitin-conjugating enzyme Ube2g2.* Proceedings of the National Academy of Sciences, 2009. **106**(10): p. 3722-3727.
91. Zheng, N., et al., *Structure of a c-Cbl–UbcH7 Complex: RING Domain Function in Ubiquitin-Protein Ligases.* Cell, 2000. **102**(4): p. 533-539.
92. Rodina, A., et al., *Identification of an allosteric pocket on human hsp70 reveals a mode of inhibition of this therapeutically important protein.* Chemistry & biology, 2013. **20**(12): p. 1469-1480.
93. Arcangeli, A. *Expression and role of hERG channels in cancer cells*. in *Novartis Found Symp*. 2005.
94. Goloudina, A.R., O.N. Demidov, and C. Garrido, *Inhibition of HSP70: a challenging anti-cancer strategy.* Cancer letters, 2012. **325**(2): p. 117-124.
95. Massey, A.J., et al., *A novel, small molecule inhibitor of Hsc70/Hsp70 potentiates Hsp90 inhibitor induced apoptosis in HCT116 colon carcinoma cells.* Cancer chemotherapy and pharmacology, 2010. **66**(3): p. 535-545.
96. Whitesell, L. and S.L. Lindquist, *HSP90 and the chaperoning of cancer.* Nature Reviews Cancer, 2005. **5**(10): p. 761-772.
97. Zhang, T., et al., *A novel Hsp90 inhibitor to disrupt Hsp90/Cdc37 complex against pancreatic cancer cells.* Molecular cancer therapeutics, 2008. **7**(1): p. 162-170.
98. Bianchi, L., et al., *hERG encodes a K+ current highly conserved in tumors of different histogenesis: a selective advantage for cancer cells?* Cancer research, 1998. **58**(4): p. 815-822.
99. Shao, X.D., et al., *The mechanism of COX-2 regulating HERG channel in gastric cancer cells.* Bratisl Lek Listy, 2014. **115**(8): p. 487-91.
100. Cicek, M.S., et al., *Epigenome-wide ovarian cancer analysis identifies a methylation profile differentiating clear-cell histology with epigenetic silencing of the HERG K+ channel.* Hum Mol Genet, 2013. **22**(15): p. 3038-47.
101. Cherubini, A., et al., *HERG potassium channels are more frequently expressed in human endometrial cancer as compared to non-cancerous endometrium.* Br J Cancer, 2000. **83**(12): p. 1722-9.
102. Guo, J., et al., *Extracellular K+ concentration controls cell surface density of I Kr in rabbit hearts and of the HERG channel in human cell lines.* The Journal of clinical investigation, 2009. **119**(9): p. 2745-2757.
103. Wu, Z.-Y., et al., *Progesterone impairs human ether-a-go-go-related gene (HERG) trafficking by disruption of intracellular cholesterol homeostasis.* Journal of Biological Chemistry, 2011. **286**(25): p. 22186-22194.